DOT/FAA/AM-19/9
Office of Aerospace Medicine
Washington, DC 20591

Pilot Performance on a SA CAT I Instrument Approach Using Synthetic Vision on a Head-up Display and a Retrofit Head-down Display

Dennis B. Beringer, Ph.D.[1]
David A. Domino[2]
Jill Kamienski[2]

[1]FAA Civil Aerospace Medical Institute
Oklahoma City, OK 73125
[2]MITRE Corporation
Center for Advanced Aviation System Development
7515 Colshire Drive
McLean, VA 22102

March 2018

Final Report

Technical Report Documentation Page

1. Report No.	2. Government Accession No.	3. Recipient's Catalog No.
DOT/FAA/AM-19/9		

4. Title and Subtitle	5. Report Date
Pilot Performance on a SA CAT I Instrument Approach Using Synthetic Vision on a Head-up Display and a Retrofit Head-down Display	September 2019
	6. Performing Organization Code
7. Author(s)	8. Performing Organization Report No.
Beringer D,[1] Domino D,[2] Kamienski J,[2]	
9. Performing Organization Name and Address	10. Work Unit No. (TRAIS)
[1]FAA Civil Aerospace Medical Institute P.O. Box 25082 Oklahoma City, OK 73125 [2]MITRE Corporation Center for Advanced Aviation System Development 7515 Colshire Drive McLean, VA 22102	11. Contract or Grant No.
12. Sponsoring Agency name and Address	13. Type of Report and Period Covered
Office of Aerospace Medicine Federal Aviation Administration 800 Independence Ave., S.W. Washington, DC 20591	14. Sponsoring Agency Code

15. Supplemental Notes

16. Abstract

Thirteen two-person crews flew SA CAT I approaches to KOKC runway 35R in a B-737-800 Level D flight simulator. Conditions were varied by: (1) display type – head-up display (HUD) w/o synthetic vision (SV), HUD w/SV, and head-down display (HDD) w/SV; (2) runway lighting – High-intensity runway lights (HIRL), HIRL plus runway centerline lights (RCL), HIRL plus RCL plus touchdown-zone lights (TDZ); (3) ambient illumination – day, night; and (4) combinations of decision height (DH) and runway visual range (RVR) – 100'/1200', 150'/1400'. Results suggest that there were no performance differences between using a head-down and the head-up synthetic-vision displays that rose to the level of operational significance pilot preferences not withstanding.

17. Key Words	18. Distribution Statement
Synthetic Vision, SVGS, SA CAT I, Pilot Performance Displays, HUD, HDD	Document is available to the public through the Internet: http://www.faa.gov/go/oamtechreports/

19. Security Classif. (of this report)	20. Security Classif. (of this page)	21. No. of Pages	22. Price
Unclassified	Unclassified	96	

Form DOT F 1700.7 (8-72) Reproduction of completed page authorized

Table of Contents

List of Tables

List of Figures

List of Acronyms and Abbreviations

Acronym	Term
AFS	Federal Aviation Administration Flight Standards Service
AGL	Above Ground Level
ALSF-2	High Intensity Approach Light System with Sequence Flashing Lights 2
CAMI	FAA Civil Aerospace Medical Institute
C/L	Center Line
CAT I	Category I
CAT II	Category II
DA	Decision Altitude
DH	Decision Height
EFVS	Enhanced Flight Vision System
FAA	Federal Aviation Administration
FLIR	Forward Looking Infra-Red
FPARC	Flight Path Angle Reference Cue
FPV	Flight Path Vector
GPS	Global Positioning System
HAT	Height Above Touchdown
HDD	Head Down Display
HIRL	High Intensity Runway Lights
HUD	Head Up Display
ICAO	International Civil Aviation Organization
ILS	Instrument Landing System
MALSR	Medium Intensity Approach Light System with Runway Alignment Indicator Lights
MIRL	Medium Intensity Runway Lights
MSL	Mean Sea Level
NASA	National Aeronautics and Space Administration
NTSB	National Transportation Safety Board
OTW	Out the Window
PAPI	Precision Approach Path Indicator
RadAlt	Radio Altimeter
REIL	Runway End Identifier Lights
RVR	Runway Visual Range

Acronym	Term
SA CAT I	Special Authorization Category I
SA CAT II	Special Authorization Category II
SV	Synthetic Vision
SVGS	Synthetic Vision Guidance System
SVS	Synthetic Vision System
TDZ	Touchdown Zone
TDZL	Touchdown Zone Lights
TOGA	Takeoff and Go Around (Missed Approach)

INTRODUCTION

Low visibility operations have been studied for several decades, with the intent of improving the ability to operate reliably and safely in these conditions to maximize the efficiency of the air transportation system. With the development of precision approach landing aids such as the Instrument Landing System (ILS), and vertically guided approaches based on the Global Positioning System (GPS), it has been possible to incrementally reduce the visibility requirements to operate to properly equipped runways, relying primarily on the ground-based navigation and runway infrastructure to support the operation. This infrastructure, especially that required for the lowest approved visibilities, is expensive to install and maintain, and thus relatively few runways have been equipped, and only at airports where the operational demand could justify the costs of installation. For example, the most recent flight procedure inventory summary lists only 41 published ILS Category II approaches, while there are over 1500 ILS Category I approaches with standard or above standard minimums.

The intent of this study was to evaluate two implementations of Synthetic Vision Guidance System (SVGS) technology: one implemented on a head down display (SVGS-HDD) and the other on a head up display (SVGS-HUD). Each was assessed during low visibility approaches to Special Authorization Category I (SA CAT I), and Special Authorization Category II (SA CAT II) ILS weather minima. SA CAT I and SA CAT II operations were developed specifically to leverage the capability of airborne equipment to enable approaches to runways with reduced lighting infrastructure that is less than current requirements. This study evaluated the contribution of SVGS to visual search and acquisition of the runway environment using both display implementations. In particular, the head down to head up transition and acquisition of the runway environment using the SVGS-HDD were evaluated, as well as the cognitive transition from attention to the displayed SVGS imagery to direct out the window (OTW) contact with natural visual references.

In SA CAT I (Decision Height 150 ft, Runway Visual Range 1400 ft) and SA CAT II (Decision Height 100 ft, Runway Visual Range 1200 ft) operations an airplane that is certified for Category II operations must be used. It must be equipped with a Category II certified Head Up display (HUD) and flown by a CAT II qualified crew. This simulation was intended to provide information regarding pilot performance that would indicate whether pilot performance using SVGS head down displays is sufficiently comparable to pilot performance using the currently approved head up displays. The full sets of current requirements for each operation are specified in FAA Order 8400.13D (FAA, 2009).

BACKGROUND

FAA announced the qualifying criteria for ILS Category II operations in 1964 (FAA, 2017); United Airlines became the first to qualify for the initial approval at a decision height (DH) of 150 feet (ft) in visibilities as low as 1600 ft runway visual range (RVR). In 1967, FAA adopted an approach light system compliant with International Civil Aviation Organization (ICAO) standard for Category II operations (ICAO, 2013). The resulting FAA standard is the High Intensity Approach Light System with Sequence Flashing Lights 2 (ALSF-2) (FAA, 2010). This system includes the ICAO standard red barrettes on either side of the approach centerline bar starting at 1000 ft from the threshold. The approach barrettes are continued into the touchdown zone (TDZ) as white lights to provide robust visual information to complete the flare and landing.

In November of 1967, Pan American World Airways was the first airline to receive approval for the current Category II standard of 100 ft DH and RVR 1200 ft. (FAA, 2017). Fifty years of safe Category II operations have ensued since that first approval. A review of the National Transportation Safety Board (NTSB) aircraft accident database disclosed a single non-fatal, short landing accident that occurred in conjunction with a Category II approach operation.

Vision Systems

Several technological advancements have made it possible to reduce the ground infrastructure requirements based on capabilities installed in the cockpit and thus expand low visibility access to more runways. The advent of GPS, and the supporting aircraft avionics, including flight directors and autopilots, have made it possible to provide precision navigation to the landing position to a far greater number of runways than would be economically justifiable for the installation of full CAT II ground-based infrastructure.

After reaching the landing decision altitude (DA) or decision height (DH), pilots must still find the runway and complete the landing visually. This aspect of the operation is now supported on some aircraft by airborne technologies known under the broad term "vision systems."

Two primary types of systems are currently in use: Enhanced Flight Vision System (EFVS) and Synthetic Vision Systems (SVS). EFVS imagery of the airport environment and the landing runway is generated in real time using forward looking infrared (FLIR) sensors and displayed on a Head-up Display (HUD). EFVS has been approved for landing credit, including operations to touchdown by sole reference to the EFVS imagery (14 CFR §91.176).

SVS provides pilots with weather-independent imagery of the airport environment derived from terrain, runway and obstacle databases, and rendered in three dimensions from the pilot eye point of view. This imagery can be displayed on the HUD or on electronic head-down displays (HDD), regardless of the prevailing weather conditions. This capability is currently only approved as an aid to situation awareness as the intended function. No operational credit is offered for equipage with SVS. It is this capability that is the focus of the present study, in an implementation known as a Synthetic Vision Guidance System (SVGS).

Synthetic Vision Guidance System (SVGS) Standards

To address the possibility of using a synthetic vision system for operational credit RTCA Special Committee 213 (SC-213) was tasked with developing performance standards for an advanced SVS that would have the accuracy, integrity, and reliability required to qualify for some level of operational credit. The SVGS standards are published in RTCA DO-359 *Minimum Aviation System Performance Standards (MASPS) for Synthetic Vision Guidance Systems* (RTCA, 2015). The system standards provide database assurance, integrity monitoring, and flight guidance and control imagery similar to that used in HUD displays. Two critical elements of the display suite are the flight path vector (FPV) cue and the flight path angle reference cue (FPARC). These two features, combined with a display of the landing runway enable pilots to monitor and control their descent path to touchdown, while display of the runway provides visual search guidance when entering the visual segment of the approach.

Previous Research

Two lines of previous research are relevant in the context of a head-down SVGS operation; they are very much related to one another regarding pilot performance during low visibility landings. The first is the relatively extensive history of research that has examined various aspects of the head-down to head-up transition

The second thread has examined the visual cues required for control of the aircraft and flight path after the transition to head-up visual operations has occurred. This would include the initial visual acquisition of the runway environment and thence through alignment flare and touchdown. This work addresses what could be broadly described as what pilots must "see to land". This information has been applied in the design of the lighting and marking requirements for instrument runways to ensure that what pilots need to see will be seen.

Head-down to Head-up transition. Pilot performance during the head-down to head-up transition has assumed obvious importance as authorized visibilities have been incrementally reduced over the past 50 years. Until the development and deployment of HUD equipment, a head-down to head-up transition was required for all low visibility operations and therefore was an important research subject. Haines (1980a and 1980b) notes that there are two components to the transition; the physical transition from head-down instrument reference to head-up visual reference (including visual accommodation), and the cognitive transition from instrument derived control information to visual control information.

Lybrand (1959) reporting on work by Garbell (1951) provides a succinct presentation of these two requirements:

> "The principal elements of pilot information are identification and guidance. The concept of 'identification' in an airport lighting and marking system is understood to include both the selective distinction of a given instrument-approach zone or runway from the respective surroundings, and an indication of the location, general direction, and sense of orientation of the runway axis.
>
> The concept of 'guidance' in an airport lighting and marking system is understood to include the information required by the pilot to visualize the location and direction of motion of the aircraft at any given point of the approach with respect to the runway upon which landing is intended. Referring to the examples of either a fog or a uniform ground surface lacking in adequate reference features ('texture,' protrusions of known height, a horizon, etc.**),** the guidance elements expected from the artificial visual aids would include the three 'location' coordinates:
>
> X **-** longitudinal distance from the runway threshold.
>
> Y **-** transverse distance from the vertical plane through the runway axis.
>
> Z **-** elevation with respect to the ground or to an ideal glide plane, together with an indication of two 'directional' guidance elements:
>
> The direction of motion of the aircraft in a horizontal plane.
>
> The attitude in bank (roll) of the aircraft."

Approach and runway lighting systems currently required for use during low visibility operations are designed to provide this information during the visual segment of the approach.

Addressing the physical component of the transition, Spady (1978) used an oculometer to track pilot gaze behavior during approach. The data collected from 500 ft above touchdown to 20ft above touchdown was analyzed in two segments: 500 ft to 200 ft and 200 ft to 20 ft. The descent time from 500 ft to 200 ft was about 25 seconds (s). The mean number of visual transitions in this period was 4.6 with a total head-up time of 2.7s (17% of total). From 200 ft to 20ft the descent time was about 15s, with pilots looking head-up for about 4.2s (39% of total). Not surprisingly, pilots clearly were shifting their attention outside as they got closer to the runway.

Dwell times for each transition were on the order of 0.8s. The very short dwell times suggest that these were quick checks to determine if *any* visual information was available since they were shorter than the time required for visual accommodation to occur. Time required for the transition leading to a landing decision was much longer as reported below.

On the issue of cognitive time required to acquire the required visual cues for aircraft control and a landing decision, Haines (1980a), reporting on work by Brown (1970) indicates that during Category II simulated night approaches, pilots who were solely monitoring for visual cues (as might be the case in a monitored approach technique) could make the landing decision in about 2s. For pilots using conventional procedures, 3s was more representative based on the 500 approaches flown in the study. Brown also noted that the landing decision occurred almost twice as fast when pilots were assessing the visual environment from 150 ft or 100 ft than when the decision was made at 200 ft, suggesting a higher likelihood of completing the landing for the lower decision heights (DH).

Haines (1980a) compared HUD vs HDD transitions and essentially replicated the Brown results with respect to the HDD runs. Haines found mean head-up transition landing decision times of about 3.5s for ceilings 300 ft or less with visibilities at RVR 2400 and RVR 1600. The number of head-up transitions by pilots was variable, ranging from 4 to 14 depending on ceiling height. Mean decision time for the lowest RVR condition (150 ft DH/RVR 1600) ranged from 2.7s to 2.0s with shorter times for lower ceilings. Swartz, Candra, and Madero (1976), reporting on work done at the Royal Air Force Institute of Aviation Medicine, indicates that the accommodation time lag was on the order of 2.4s. There was no correlation found between landing performance and any of the visibility/DH conditions and all landings completed successfully once the landing decision had been made. Haines also notes the possible issues that may arise with pilots whose eye focus times are relatively long as they transition from instrument to outside visual cues.

With respect to flight path control Haines (1980a) reports interesting findings that are relevant to the present study. All approaches in his research were flown with autopilot engaged. However, several planned “unexpected” disconnects were inserted into the scenarios to evaluate flight path control under that circumstance. There was no difference in final segment and landing performance between HDD and HUD autopilot disconnect scenarios, except for smoother throttle control in the HUD condition. The smoothness of the manual takeover to landing was determined to be equivalent for the two displays.

See to land. Once the head-down to head-up transition has occurred the pilot must still locate the runway and then complete the final alignment, flare, and landing. The available visual cues must be of sufficient quality to perform these tasks. Substantial research has been completed to define the minimum visual information requirements.

A review study by Swartz et al. (1976) and colleagues reported on research conducted by the Air Force to determine the lowest weather conditions under which manual landings could safely be conducted, with an emphasis on pilot human factors related to aircraft control in the visual segment and the decision to land. The study identified the same primary perceptual factors noted by Garbell (1951), lateral guidance information and vertical guidance information. Lateral guidance was judged to be much easier, requiring a visual segment of about 600ft to 800ft. When considering a cockpit cutoff angle of 14º, this would require RVR 1200 visibility. The type of approach lighting used was not reported.

Swartz et al. (1976) also reports that "…reliable visual vertical control of an aircraft begins only when the pilot can see discreet [sic] and identifiable points such as the runway threshold, and does not fully develop until he can see the projected touchdown point". For vertical control, a visual segment of 1200 ft was judged necessary, suggesting a visibility of RVR 1600 to account for cockpit cutoff angle. The practical requirement of these factors is that a source of vertical guidance information in pitch seems to be required to at least 100 ft to offset the tendency to duck under the desired glideslope during the transition to visually controlled flight.

Eversmeyer, Reisweber, Liao, and Avery (2008) reporting on a demonstration of ILS approaches in CAT I and CAT II weather conditions observed the same phenomenon. Descent rate, airspeed deviation from 500 ft to threshold, and touchdown footprint were used as performance criteria. Six airline crews participated as evaluation pilots. Approach methods were a mix of hand flown using flight director, hand flown using HUD, and coupled approaches using flight director and autopilot. In the 5 hand-flown scenarios (30 approaches), glideslope tracking data and debrief comments both suggest evidence of duck under behavior. Twelve of the 30 approaches produced violations of the descent rate test criterion, although the subsequent landings were within the designated touchdown footprint.

Recent Research with Vision Systems

The prior early research indicates that the head-down to head-up transition takes several seconds, involves both physical movement and cognitive accommodation of the visual system, and is not consistent with respect to lateral and vertical perceptions of the flight path. Perceptual errors in vertical flight path judgment have been known to contribute to incidents and accidents. In addition, the currently approved visibilities for Special Authorization Category I (SA CAT I), and Special Authorization Category II (SA CAT II) approaches (see Figure 1), preclude the direct visual contact with the approach aim point or even the threshold, which have been shown to be necessary for reliable, purely visual control of the lateral and vertical flight path.

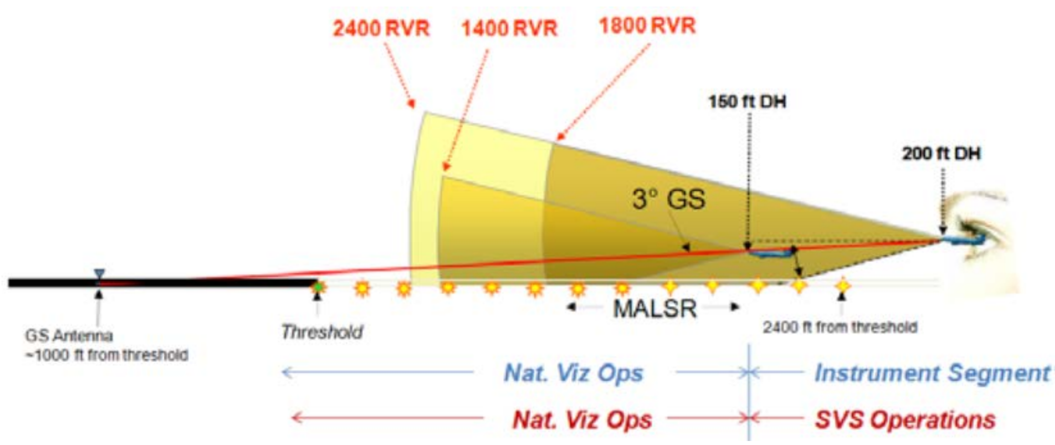

Figure 1. Illustration of visibility limits for standard CAT I and SA CAT I operations.

Even when using normal instrument approach minima (DH 200 ft, visibility 2400 RVR) neither the threshold nor the touchdown aim point will be visible. At the 200 ft DH the airplane is about 2800ft from the threshold and 3800ft from the touchdown point. Reduced visual segments in low visibility are a well-known contributor to the “duck under” phenomenon in which pilots misperceive that they are above the glide path when reduced visual cues first come into view. This is not a new phenomenon; Calvert and Sparke (1958) reporting on work at the Royal Aircraft Establishment, noted that in low visibility conditions short visual segments often resulted in pilots descending below the ILS glideslope.

Fortunately, the system capabilities of vision systems address some of these perceptual limitations in a variety of ways, and a substantial body of research has been completed to evaluate the ability of such systems to support low visibility operations.

The work of particular interest to the present study is focused on approach stability in the visual segment, landing touchdown performance, and whether head-down presentation of visual imagery can contribute to pilot performance during the visual segment from the DH to touchdown. A system design including instrument approach procedures, flight deck procedures, and new display capabilities may reduce the times required for visual acquisition and may improve the reliability and safety of the operation.

The National Aeronautics and Space Administration (NASA) has performed a series of studies examining various aspects of vision systems including assessment of pilot performance in the visual segment. Kramer, Williams, and Bailey (2008) evaluated two display modes (HDD and HUD), with and without synthetic imagery. Three levels of runway infrastructure were evaluated:

Basic VFR (runway end identifier lights (REIL), partial threshold lights, precision approach path indicator lights (PAPI), and medium intensity runway lights (MIRL)

Category I MALSR (medium intensity approach lights with runway alignment indicator lights, threshold lights, REIL, PAPI, MIRL)

Category II ALSF-2 (high intensity approach lights, sequence flashing lights, touchdown zone lights (TDZL), runway centerline lights (C/L), threshold lights, high intensity runway lights (HIRL)

Four visibility levels (3 miles, 2400ft, 1800ft, 1200 ft RVR) and two decision altitudes (200 ft, 100 ft) were assessed. Of particular interest are the runs using the Category I MALSR configuration (edge lights only, no TDZ or C/L lights) at 1800 and 1200 RVR, since this closely matches one of the test conditions in the present study.

Objective performance, situation awareness (SA), and workload data were collected for all tested conditions. Performance standards for comparison were drawn from four sources, the FAA Instrument Pilot Practical Test Standard, AC 120-29 Criteria for Approval of Category I and Category II operations, FAR 14 CFR §91, and the European Joint Aviation Regulations–All Weather Operations AMC AWO 231.

Pilots reported the lowest workload and highest SA when using the HUD with SV imagery (SV-HUD). The pilot workload associated with the SV-HDD and the Baseline-HUD (no imagery) was rated by the pilots as being equal. The SA when using the SV-HDD was rated significantly better than the Baseline-HUD.

Pilots had statistically less localizer deviation when flying the HUD (mean=0.060 dots and standard deviation, σ=0.036) compared to the HDD (mean=0.068 dots and σ=0.029). The presence or absence of SV imagery was not significant. Note that the .008 dot angular difference may not be visually perceptible and is well within the AC 120-29 Category II performance standard of .667 dots deviation.

Glideslope performance was more variable, with the HUD conditions yielding less deviation. Objective performance to the 100 ft DH with HUD was a mean=0.270 dots and σ=0.141, compared with the HDD mean=0.366 dots and σ=0.188. However, both values are well within the AC 120-29 standard of 1.0 dots deviation

Irrespective of glideslope tracking, actual landing touchdown performance with all display modes was within the lateral and acceptable sink rate standard for CAT II auto-land requirements. There were statistical differences found between RVR condition, approach light system, and decision altitude, but the differences were judged not operationally significant.

In a follow-on study, Kramer et al. (2013) conducted an evaluation of synthetic and enhanced vision concepts for terminal area, approach, and surface operations. The approach portion of the study directly assessed the use of SV imagery on HUD and HDD displays in weather conditions replicating existing SA CAT I and proposed SA CAT II authorizations (RVR 1400 and RVR 1000 respectively). Of interest for the present study is their results in SA CAT I conditions (RVR 1400). Two head-down (Baseline and SV) and three head-up concepts (Baseline, SVS, and EFVS) were evaluated using “monitored approach” procedures. Crosswinds up to 15kts were randomly assigned to approaches. Two runway lighting conditions were evaluated, TDZ and CL, both on or both off. Assessment of CL only was not included. Edge lights were available for all approaches. Performance data on path errors, descent rates, and touchdown footprint were collected. Pilots assessed workload and situation awareness (SA) after each approach. The primary dependent variables for this study were focused on landing performance, including deviation from runway centerline at touchdown, along track distance from threshold, sink rate, and containment within the CAT II auto-land footprint being used as the default standard for acceptable performance. Analysis of path error was not reported.

Results showed that all display concepts showed relatively small lateral deviation from the centerline at touchdown. No statistical or practical differences were noted between the evaluated display conditions. Longitudinal touchdown points for SV HDD configuration was in the “acceptable” or “adequate” range for all approaches ending in landings (20 of 24 approaches), irrespective of runway lighting (TDZ/CL) condition. The “adequate” range included the full length of the CAT II auto-land footprint (200 ft to 2700ft from threshold), while the “desired” range was tighter (750 ft to 2250 ft from threshold). Pilot reported workload for the SV HDD condition was judged by pilot flying (PF) and pilot not flying (PNF) as “moderate, easily managed, and having considerable spare time”. Comparing HDD SVS to HDD without SVS in these same conditions (1400 RVR), SVS provided a reduction in missed approaches (TOGAs) (7 TOGAs vs. 4) likely by providing an aided search for the pilots; they knew where to look for the runway and may have had better awareness of the situation approaching the DH.

Ellis, Kramer, Shelton, Arthur III, Norman, and Prinzel III (2011) and Ellis et al. (2012) performed a study to validate the performance of the SmartEye tracking system, which used SVS operations to more fully explore instrument to visual transition behavior, including the head-down to head-up transition when using HDD. The researchers used eye/head tracking data to infer pilot attention and record visual behavior. The evaluated variables included percentage of head-up time, head-down to head-up transition count, and for the HDD conditions the altitude at which the first transition glance occurred. Two comparisons are of interest: baseline HUD to SV HDD, and SV HDD to baseline HDD, particularly during the instrument to visual transition. Five eye tracking analysis segments were identified, including Instrument, Instrument to Visual, Visual, Flare, and Landing. Four display types were used, HUD with SVS, baseline HUD, HDD with SVS and baseline HDD.

Eye tracker performance was robust and good data were collected. Of interest to the present study was the Instrument to Visual Transition and Visual Segment data. The researchers found that, not surprisingly, the HUD conditions (both with SV and baseline) resulted in the highest percentage of head-up time during the instrument to visual transition. There was no statistical difference in head-up time between the SV and baseline percentages (87% to 98% for baseline, 91% to 99% for SV).

In comparing the two HDD conditions, the findings indicate that with SVS the head-up to head-down transitions account for 30% of the head down time suggesting that pilots are still flying the guidance on the SVS display in the visual segment and not merely referencing it. This is in keeping with the early findings of Swartz et al. (1976), which proposed that having the runway threshold and touchdown point in view were requirements for solely visual control, especially in pitch. In addition, pilots flying with SVS made their initial glance up to OTW at a lower altitude closer to DH than with baseline and were also lower at full transition. The researchers hypothesized that this indicates a more decisive transition to OTW when using a SV-HDD, suggesting greater confidence in their trajectory and where to find the runway, resulting in more efficient visual behavior.

Kramer et al. (2013) report on a comprehensive simulation study conducted to evaluate the operational feasibility of conducting a straight in instrument approach using HUD-based EFVS to touchdown with RVR 1000ft, and an SVS HDD to a DH of 150 ft at 1400 RVR, then transitioning to natural out the window (OTW) cues to complete the landing. 24 evaluation pilots were used, ten crews flew for U.S air carriers and the remainder for business aircraft operators. Since all conditions were flown within subjects, all were required to have previous HUD experience.

For purposes of the current study, one important comparison was pilot performance using the baseline HUD with no imagery and pilot performance using the HDD with SVS imagery, with both operations conducted to the SA CAT I limits of DH 150 ft and visibility RVR 1400ft. The runway was equipped with a MALSR approach light system, but not with centerline lights or touchdown zone lights. Pilot gaze was evaluated using an unobtrusive eye tracking capability.

The findings show that:

During the visual segment of flight (from the DH 150 ft HAT to touchdown), the SVS HDD condition pilot visual attention remained inside the flight deck 25% of the time, replicating the findings of Ellis et al. (2011 and 2012). Pilot visual attention continued to transition between the OTW scene and the HDD. However, compared to the conventional HDD condition, head-up time was 10% greater when using the SVS HDD during the visual segment.

The data show no statistically significant differences due to the presence or absence of SVS on the HDDs when comparing a pilot's first transition to OTW to find the visual references/landing runway.

However, comparing all transitions, the data do indicate better performance for SVS, with 82% of the transitions in the correct direction to the runway vs. 73% correct without SVS. For the full transition to visual flight (the time when the pilot goes head-out and stays predominately head-out for landing), the presence of SVS also supported a more accurate transition. The pilot using an HDD with SVS correctly looked in the proper direction for the runway 87% of the time, versus only 66% of the time without SVS. Wind correction angle and resulting offset of the displayed runway were not reported.

SVS HDD decreased the head-down time during the visual segment to an average 25% compared to 35% head-down with the Conventional HDD concept, with no significant variation in number of transitions.

With respect to landing performance comparison of the SVS concepts and Conventional HUD condition, the data show no statistically significant differences in longitudinal and lateral position or sink rate at touchdown for any of the display concepts. However, on two approaches with SVS HDD the touchdowns were short of the CAT II autoland touchdown footprint: one short of the 200 ft point in 1400 RVR conditions with centerline and TDZ lights off, and the other short of the threshold in 1800 RVR conditions with centerline and TDZ lights on. The flight crew was unaware that they landed short of the threshold.

During post flight debrief 6 of 12 pilots commented on obscuration of the landing runway by the SV imagery during SV HUD approaches, and the need to use the declutter capability to see the runway. One pilot "…could not see the lights through the SV so went around most times." One pilot seemed willing to take the landing to touchdown using the SV imagery. Another said that with IR or SV imagery available actual visibility was not relevant. In either case, the researchers noted that rendering of the SV image must be carefully designed to preclude actual obscuration of the landing cues.

The researchers also suggested that future studies should include motion-based simulation testing for the SVS HUD and HDD concepts to assess its impact on approach and landing performance, especially in sink rate control at touchdown.

Korn, Lenz, and Biella (2007), report on a series of simulator studies using an HDD to display simulated FLIR imagery in lieu of HUD. While this technology is not directly applicable to SVGS, the relevant comparison is the use of a head down display rather than HUD to display the imagery. The first study used a conventional ILS approach to demonstrate the concept. There was no difference found in performance between the HUD with FLIR imagery and the HDD with FLIR imagery procedures. Pilots flying head-down with imagery from the DH down to the visual transition height (100 ft height above touchdown (HAT) reported no difficulty in identifying the runway in the external view after transitioning from head-down to head-up. The researchers report that depiction of the runway in the imagery guided pilot visual search to the right location to look for the runway in the outside view. The non-conformal presentation of the head-down imagery did not distract from looking at the right direction in the outside vision after transitioning from head-down to head-up. Localizer and glideslope tracking performance for 48 approaches from 1000ft to 75ft HAT was good, with mean localizer deviation of 0.189º (standard deviation 0.019º), and mean glideslope deviation 0.14º (standard deviation 0.016º), well within the Category II deviation standards.

In a concluding study, Korn, Biella, and Lenz (2008) extended this work using a non-precision VOR approach. In this case, the ability of pilots to maintain a normal descent to the touchdown zone using only the imagery and without external guidance was assessed, as authorized in 14 CFR §91.176. Both HUD and HDD trials were included in the study. Wind conditions included a 10kt direct headwind and a 15kt quartering headwind, yielding a small wind correction angle of about 4º. Again, for purposes of the present study the relevant finding was the presence of a distinct bias below the nominal descent path apparent in the data, and how the pilots chose to use the available display cues. Post flight debriefing disclosed that pilots were using the runway threshold as the desired aim point for the FPARC and FPV rather than a point further down the runway at the normal touchdown zone. In post-flight discussion, pilots commented on the need for adequate training, and a strong preference for vertical guidance below the DH. This reinforces the requirement for integrated training on the interaction between displayed runway imagery and descent path management cues (FPV and FPARC), and the importance of the basic localizer and glideslope guidance, even when operating below the DH. Despite the observed below-path profiles, pilots reported no issues with the head-down to head-up transition, and all landings were completed safely.

While the previous studies focused on air carrier pilots and transport category airplanes, other research has been done with general aviation (GA) pilots and airplanes. Beringer (2016) evaluated use of SV imagery by GA pilots in a simulation study using a single engine general aviation airplane simulator (Piper Malibu). A within-subjects design was employed with each pilot flying all combinations of variables. These included display location (HUD and HDD), SV imagery (present or absent), baseline displays (round dial or PFD without imagery), runway visual range (1200 ft or 1400 ft), and decision height (100 ft and 200 ft). A separate task included an approach to a terrain challenged airport was also flown, but that work is not relevant to the present study. Dependent measures were localizer and glideslope tracking and frequency of missed approach for the SA CAT I trials.

Pilots flew 11 approaches with the different displays, one with each baseline configuration, one with reference round-dial configuration, and the others with combinations of SV with HUD and HDD. The results showed that localizer and glideslope tracking error showed no significant differences between display types. This was expected since the error indices on each display were the same, and SV imagery is not a guidance element.

With respect to completed approaches, there was a significant difference in completion rates related to DH, with more approaches completed with the 100 ft DH than the 150 ft DH. In the 1200RVR condition with 150 ft DH, pilots were equally likely to land or to miss the approach, with the pilots that landed able to do so because they overshot the DH to a lower altitude on descent.

Summary of Research Findings

The previous research has illuminated several factors of interest for the present study.

The use of HUD equipment has shown benefit in reducing the adverse performance effects of the head-down to head-up transition.

When using HUD, approach stability in the visual segment after the transition from instrument to visual control of the aircraft is improved.

The addition of SVS imagery to the HUD has been well received by pilot subjects, with some caveats related to obscuration of landing cues

Depending on the rendering method used, SVS imagery on the HUD may hinder visual search OTW. In one study 6 of 12 pilots commented that SVS imagery masks the OTW view of the runway, and decluttering was required. Additional research on clutter and masking effects was suggested.

Flight technical error using SV HUD is better than that achieved with HDD and well within CAT II limits

Flight technical error using SV HDD is also largely within CAT II performance limits

Workload using SV HDD was acceptable

Reported glideslope tracking performance for SV HDD is variable. In some studies, there was no performance difference using SV HUD and SV HDD and both fell within CAT II performance standard; in another study, glideslope performance using SV HDD was at the standard on 85% of approaches.

Comparing all head-up transitions using SV HDD, the data indicate better performance for SVS, with 82% of transitions in the correct direction to the runway vs. 73% correct without SVS.

Head-down to head-up transition behavior indicates that pilots remained head down until closer to the DH when using SV on a head down display. This suggests that SV-HDD supports a more decisive transition to visual cues with SV HDD yielding more efficient visual behavior, possibly through increased confidence that after the transition the runway would be visible.

Total time head-up was increased by 10% using SV HDD

The presence of CL/TDZ lights appears to have aided pilots in landing closer to the touchdown point but did not statistically affect the likelihood of completing the landing

Overview

The present study concentrated on two primary questions related to the use of SVGS for the approach phase. The first was related to assessing pilot performance in visual acquisition of the runway as a function of the type of display platform used. It was anticipated that guided visual search facilitated by the SV imagery could help make the visual search during transition from SVGS-HDD, instrument-referenced aircraft control to aircraft control using available visual cues more precise or expedient. In the case of SVGS-HUD, the combination of 1:1 overlaid SV imagery and command guidance could enhance transition to natural visual cues.

The second question was how much variations in runway lighting would contribute to or affect pilot performance with a specific focus on reduced lighting infrastructure. This was specifically related to whether SVGS could be used to compensate for the lack of some runway lighting features and allow the pilot to safely transition to landing, given that piloting during the visual segment would continue to rely on natural vision and pilot judgment to complete alignment, flare, and landing.

METHOD

Experimental Design

Independent variables. The variables manipulated were chosen from among those most likely to affect the pilot's ability to visually acquire the landing runway, perform the final alignment, and land the aircraft. These variables were expected to possibly have an influence on the pilot's ability to both maintain a stabilized approach within the expected Category II deviation requirements (FAA, 2009) and to complete the landing. Of particular interest was variation in the runway lighting systems that are typically used on runways served by instrument approaches. The variables and levels of those variables chosen are listed below:

Display type (A; 3 levels):
(1) Head-up Display (HUD) without SVGS (baseline)
(2) HUD with SVGS
(3) Head-down Display (HDD) with SVGS

Runway lighting (B; 3 levels) (each was added to Medium Approach Light System with Runway Alignment Indicator Lights (MALSR) used as the baseline:
(1) High intensity runway lights (HIRL; edge lights) only
(2) HIRL plus runway centerline lights (RCL)
(3) HIRL plus RCL plus touchdown zone (TDZ) lights

Ambient illumination (C; 2 levels):
(1) Day
(2) Night

Decision Height (DH)/Runway Visual Range (RVR) combinations (D; 2 levels):
(1) DH 100 ft/RVR 1200 ft (SA CAT II)
(2) DH 150 ft/ RVR 1400 ft (SA CAT I)

The two latter variables were included for different reasons. Ambient illumination can be thought of more as a sampling variable used to span the illumination conditions likely to be encountered during operations. It is thought that runway lighting is more likely to be visible sooner during night-time conditions than during day conditions. It also allowed a comparison of performances attainable using the different lighting configurations during both day and night. The combined variable, Decision Height/Runway Visual Range, was intended to represent the current SA CAT I (150/1400) and SA CAT II (100/1200) DH and RVR requirements. The design is represented in matrix form in Table 1.

Table 1. Independent variables in the context of the fully-crossed factorial design.

		Illumination (C)			
		Day – (1)		Night – (2)	
		Decision Height/Runway Visual Range (D)			
		100'/1200' – (1)	150'/1400' – (2)	100'/1200' – (1)	150'/1400' – (2)
Display type (A)	Runway Lighting (B)				
HUD – (1)	HIRL – (1)	*	*	*	*
	HIRL +RCL – (2)	*	*	*	*

	HIRL +RCL+TDZ – (3)	*	*	*	*
HUD w/SV – (2)	HIRL – (1)	*	*	*	*
	HIRL +RCL – (2)	*	*	*	*
	HIRL +RCL+TDZ – (3)	*	*	*	*
HDD w/SV – (3)	HIRL – (1)	*	*	*	*
	HIRL +RCL – (2)	*	*	*	*
	HIRL +RCL+TDZ – (3)	*	*	*	*

NOTE: HUD = Head-Up Display; HUD w/SV = Head-Up Display with Synthetic Vision; HDD w/SV = Head-Down Display with Synthetic Vision.

HIRL = High-intensity runway lights. RCL = runway centerline lights. TDZ = touchdown zone lights.

Other factors. Crosswind was used as a *sampling variable* to represent the maximum allowable direct crosswind component for the approach, from left and right, and this was systematically varied through 4 different orders of presentation to be balanced across the cells of the main design. The crosswind created a small, as it turns out, discrepancy between the pilot's view out the window and the depiction of the runway environment on the head-down display. This discrepancy is essentially the difference in angular displacement of the runway image (displaced less on the HDD, due to the HDD not being a 1:1 mapping, in terms of scale, to the contact visual image). Thus this provided a situation, in 36 of the 39 approaches, to assess how well the pilot could visually acquire the runway during visual transition when the runway was not aligned with the heading of the aircraft.

The baseline condition (3) embedded within the design (HUD w/o SV) was based on the existing low visibility authorizations provided in FAA Order 8400.13D, specifically Special Authorization Category I (SA CAT I) and Special Authorization Category II (SA CAT II) approaches. The SA CAT I approach is flown to lower DH and visibility than standard CAT I, while SA CAT II is flown to the CAT II DH and visibility, but to runways that are not equipped with full CAT II infrastructure. Both operations currently require the use of a head up display (HUD) to the published DH, and in the case of SA CAT II, use of an auto-land system *or HUD* to touchdown.

The three baselines were identical regarding the conditions (HIRL, Day, 150/1400, no wind) but one each was flown with each display platform. The trials were spaced such that one was near the beginning, one near the middle, and one at the end of the session. This allowed (1) a separate comparison of this common condition across display platforms, (2) a check on potential learning occurring during the study, and (3) a means to compare, with albeit a smaller sample of trials, wind versus no-wind conditions.

Dependent variables. Aircraft/pilot-performance variables were collected digitally and included latitude, longitude, altitude above mean sea level (MSL) and above ground level (AGL), pitch, roll, heading, airspeed, vertical velocity, localizer deviation, glideslope deviation, and weight on wheels (ground contact). From these, it will be possible to derive touchdown point/footprint, threshold crossing height, approach stability beyond the DH, and other metrics of interest.

Video/audio recording was used to capture real-time commentary from the pilot participants as well as their overt actions during the approaches and served as a back-up to the notes collected by the test administrators.

Participants

Thirteen two-person crews were used, each pair consisting of pilots selected from the same commercial carrier to ensure a common understanding of standard operating procedures. They were recruited for the research effort by a contractor who had provided crews to the FAA for previous research in this type of simulator. Each individual was currently qualified in the B-737 Next Generation (NG) aircraft and the captains were qualified for HUD operations. All captains were males, 2 of the FOs were females. Demographics for these individuals will be concerned mainly with the pilot flying, as they were the only pilot manipulating the controls and making decisions about continuing the approach to landing. A brief summary of the sample statistics for pilot flying follows in Table 2.

Table 2. Demographics for pilots flying.

		Range	
Demographic Measure	***Median***	***Minimum***	***Maximum***
Year began licensed flying	1987	2006	1971
Age	56	44	63
Hours last 90 days	187 (mean)	75	250

Procedure

Facilities/Equipment. The study was conducted at the FAA simulation facility at the Mike Monroney Aeronautical Center, Oklahoma City, in the B-737-800 Level D simulator (operated by the Flight Operations Simulation Branch) with displays augmented to provide both HUD and HDD presentations of synthetic-vision imagery. The simulator was operated with the motion on. The head-down display simulation was achieved by creating an external SV display on a high-end rack-mounted personal computer (PC), connecting the output of key variables from the 737 simulator to the PC, and then porting, resizing, and cropping the display image to fit on the native PFD glass on the captain's side of the cockpit, which is a square display approximately 6 5/8 inches on a side (for comparison, the G-1000 PFD as installed in the Cessna Mustang is approximately 6.5 inches tall by 8.5 inches wide, but is smaller than some other fielded EPFDs) . The display was also designed to display the RadAlt DH setting entered by the captain along with some approach alerts. The simulated SVGS display features and capabilities and flight-technical-error annunciations were compliant with the requirements in RTCA DO-359. The key SVGS features of terrain, runway display, flight path vector (FPV) and flight path angle reference cue (FPARC) were included, as well as the normal flight-control information (pitch and roll references, barometric altitude, airspeed, vertical velocity, radio altitude, flight-director cue, ILS raw-data indications). The SVGS-HDD imagery was rendered in color, while the SVGS-HUD, displayed on the already installed HUD but using a version of the software that generated SV, was limited to monochrome green (HUD capability). While color imagery is not a MASPS requirement for HDD, no known implementation of SVS displays uses a gray scale or monochrome (green) representation for terrain and runway imagery on a head down display. The first officer had the conventional 737 instrumentation (no HDD SV repeater) and did not use the HUD on that side (one was installed but it remained stowed). A photograph of this display is presented in Figure 2. For comparison, Figure 3 depicts the 737 HUD with Synthetic Vision enabled.

Figure 2. Electronic PFD, head-down, with Synthetic Vision elements, flight director, flight-path marker, and other key elements.

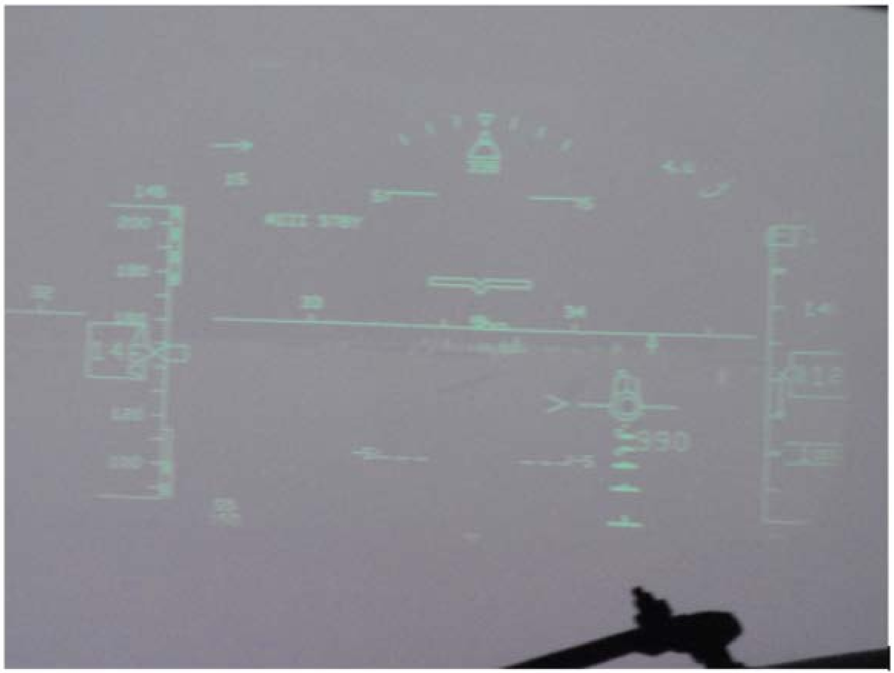

Figure 3. Actual photograph through HUD from 737 flight simulator in simulated IMC.

Following the HUD practice/training, and prior to the use of the HDD, the pilot flying was shown, at one mile from the threshold, how the runway would appear on the HDD with a 5-degree deflection of aircraft heading from runway heading (simulating crosswind tracking) and with the out-the-window view full IMC so that no runway was visible. Next, in the sequence termed “Where’s Waldo” by the experimenters, the pilot flying was asked to point to the location out the window where the runway should be. The visibility was then increased to “unlimited” so that the pilot could see how well the estimate of the location correlated with the actual location of the runway. This was done once each for plus 5 and minus 5 degree heading deflections. An additional repetition was used if requested by the pilot. The HDD practice also used a minimum of two trials and to the same criteria. This was intended to (1) eliminate potentially large learning effects in the first few experimental trials and (2) provide some measure regarding how quickly or how well the participants adapted to using a display with an SV background. Exit from the familiarization trials was based solely on flight technical performance unless a pilot expressed the desire to continue practice trials due to being unduly uncomfortable executing the procedure with the head-down display.

Pretest Briefing. Participants were provided, upon their arrival, an Informed Consent form that described their responsibilities and rights regarding task performance, a brief description of the task, and participants’ ability to halt the session at any time. Following their agreement to participate (signing of form), each pilot completed a short pilot-experience assessment (see Appendix A). Participants then received the normal safety briefing regarding operation of the 737 flight simulator, fire-suppression equipment, and the exit procedures for emergencies that require leaving the simulator or leaving the building. They also received a detailed explanation of the things that would be varied during the study (runway lighting, RVR, DH, display platform) and were shown images of the displays to be used. Additionally, a graphical representation of the implications of display minification was shown to the participants, depicting how the just-under 3:1 compression ratio in the head-down display would present lateral displacement between the runway image on the HDD and the runway as seen out the window. The participants were then encouraged to ask questions about any of the materials presented and about the tasks to be performed.

Warm-up/familiarization training. Each crew was allowed several warm-up trials to become familiar with the flight simulator and the displays, as well as the procedures that they will use when flying the approaches. This initially consisted of 2 HUD trials, one without Synthetic Vision (SV) and one with SV. This was subsequently increased to a minimum of two consecutive trials using HUD with SV that had to be performed per the requirements of the PTS.

Experimental Flight Task. Each crew flew 39 approaches to runway 34R (SA CAT I and SA CAT II approach, Figure 4) at KSEA (Seattle-Tacoma). The trials included each combination of the prescribed display platforms, DH/ RVR, runway lighting, and ambient illumination as defined in the experiment matrix (36) along with the three no-wind conditions (3). The simulator was fully configured for the approach at the beginning of each trial and at an appropriate airspeed, starting (released from freeze) at approximately 3 miles from the threshold and at approximately 1000 ft AGL. Prior to release from freeze crews were briefed on the current wind direction and velocity, and visibility. The simulator was then released and the crew hand flew the aircraft (autopilot and auto throttle were not used) on the approach to either a landing or a go-around. The first officer (FO) was NOT allowed to assist the pilot flying with manual control of the aircraft nor was the FO allowed to assist in visually acquiring the runway environment. The FO was, however, asked to conduct the normal callouts used by the carrier for which the particular crew flew.

Trials were in one of four counter-balanced orders to evenly distribute any order effects. Orders 1 and 2 were mirror images of one another, and 3 and 4 mimicked 1 and 2 but had the directions of the crosswinds switched from those in 1 and 2. Per the procedure used in other recent studies, the test conductor (from CAMI) in the simulator cab monitored, announced to, and confirmed with the AFS-440 simulator operator which condition was the current one to be run from the shared list of trials. The simulator operator initiated the trial, and the test conductor and an observer recorded observations of the pilots' comments and behaviors during the simulation run. An approach typically required approximately 1:41, and start-to-start cycle times for the trials varied from 2.5 to 3 minutes. Breaks were taken after trial 13 and after trial 30 if the pilots elected to take the second break.

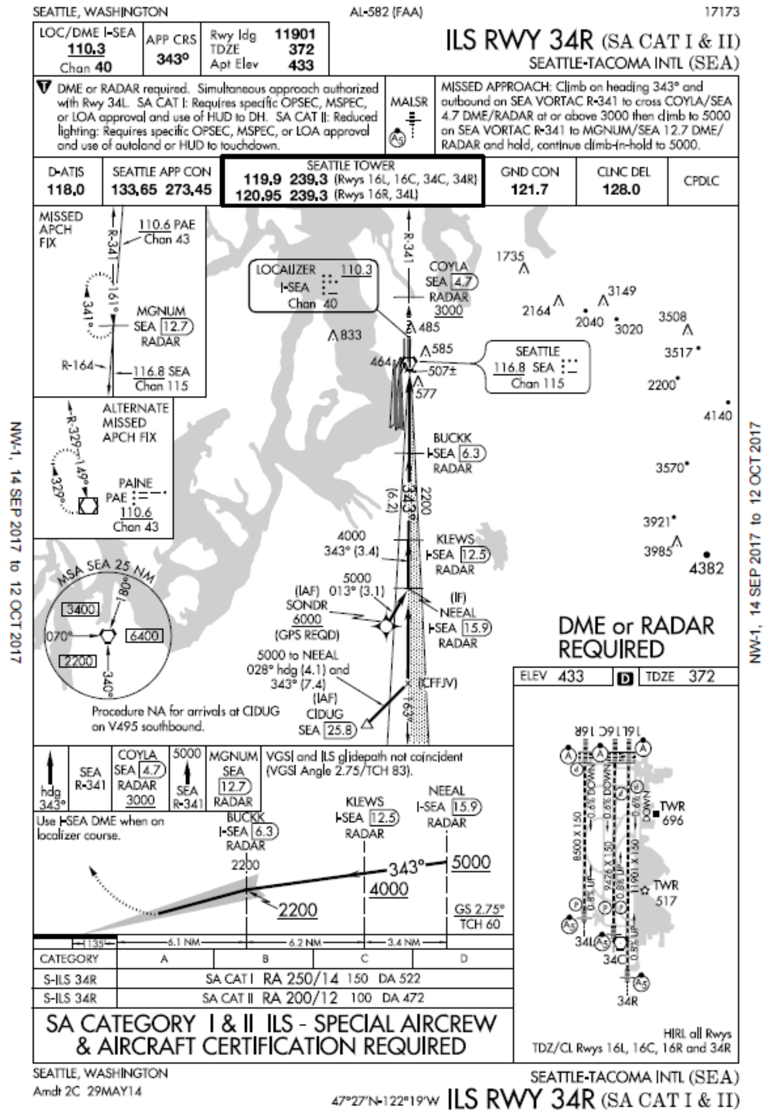

Figure 4. KSEA SA Category I and Category II ILS Runway 34R approach procedure chart.

Post-test Approaches. In some of the latter series, the pilot flying was allowed to fly one or two approaches with an HDD that had a slightly enlarged flight-director symbol, and comments were recorded concerning whether this small increase, something that had been mentioned as desirable by a number of the pilots, was in any way perceived effective. Immediately following these approaches, the FO was "rewarded" for their participation by being allowed to fly one or two approaches with SV on the HUD on their side of the aircraft.

Post-test interview. Participants completed a post-test structured interview, upon exiting the flight simulator, to record their impressions/attitudes regarding the perceived impact of the SVGS imagery and the display platforms on their flight performance. Copies of the posttest forms are included in Appendix B. The total time for a crew to complete the experiment session, preflight briefing through posttest interview, was usually less than 4.5 hours.

RESULTS AND DISCUSSION

A number of topical areas were included in the evaluation of pilot performance and preference. These included assessing the effects of the independent variables on flight technical error (touchdown point, touchdown vertical velocity, glideslope, and localizer tracking, missed approaches), training trials required, correlations of pilot experience with pilot performance, pilot opinion data (ratings of the various displays and their components, willingness to use the different displays under different meteorological conditions, preferred training method), and any unique circumstances revealed by the trials.

Touchdown point and vertical velocity

Of all the trials conducted, 7 of the 507 experimental trials resulted in a missed approach. In these cases, crews were instructed to initiate a climb (positive rate) but not to retract the gear or flaps (left down in preparation for the next trial) and the trial was terminated. The remaining 500 trials were then examined initially by plotting the touchdown points and vertical velocities at touchdown (calculated by subtracting RadAlt at touchdown-400 msec from RadAlt at touchdown-200 msec). Two graphics of these touchdown points are presented in Figures 5 and 6. Figure 5 depicts an overhead view of the runway showing the lateral dispersion of the touchdown points (color-coded by crew). Figure 6 shows this same distribution as seen from abeam (to the east of) the runway near ground level and directly across from the VOR and just north of abeam the PAPI (height of posts represents relative vertical velocity) to provide an overall sense of how the vertical velocities were distributed. One can also see that crews (in reality, the performances of a captain) tended to group together, particularly where there were “extreme” positions registered. It should be kept in mind that these distributions by geographical placement are limited by the accuracy with which Google Earth displays lat/long coordinates and should be considered only illustrative and not as a source for detailed analysis.

Figure 5. Distribution of touchdown points coded by crew and vertical velocity.

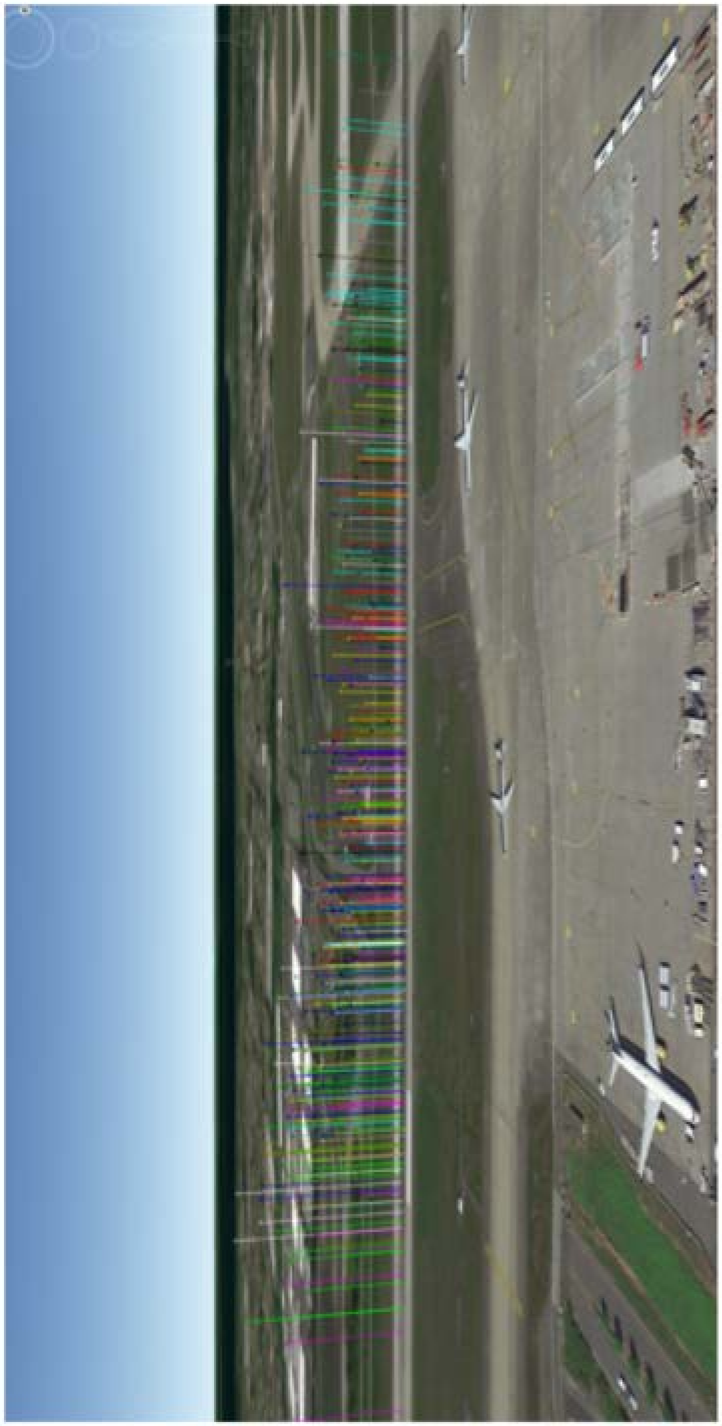

Figure 6. Touchdown points coded by crew (color) and vertical velocity (line heights).

Mean (average) error. Four-factor analyses of variance (ANOVA) were performed to determine what effects the independent variables had on bias (mean) error for touchdown point (longitudinally, as measured by distance to touch-down zone; defined in the data source, flight simulator, as distance from the aircraft to abeam the PAPI lights; laterally as measured by distance to runway centerline) and descent rate immediately prior (200 msec) to touchdown. The first two measures were taken directly from the dataset. Vertical velocity could not be taken directly from the value "vertical velocity" in the dataset for two reasons: (1) the value at aircraft-on-ground status was influenced by compression of the gear struts (modeled) and thus represented a reduction from the in-air rate and (2) the value obtained at the last sample (200 msec) before the aircraft was registered on ground was in a few cases positive (indicating a climb), which was clearly not consistent with physics. This was hypothesized to be a function of an aggressive flare and the static port being modeled as on the nose of the aircraft, in which case it would theoretically be possible to have the static port actually elevating slightly immediately before ground contact. As such, RadAlt (believed reliable when over the runway) was used and the difference between the last two samples before ground contact (touchdown minus 400 msec and touchdown minus 200 msec) was used to calculate a vertical rate in feet per second.

Some cases had to be removed because of the missed approaches and thus no ground contact. However, this then caused an imbalance in sample size between some cells. In order to maintain an equal-n analysis, some parallel cases and, in some cases sets of approaches, had to be removed, only from this specific analysis.

The results indicated that only three main effects of average error were statistically significant. These were the effect of ambient illumination (day/night) on Distance to Touchdown Zone center [$F(1,8) = 6.25$, $p = .037$)], the effect of Display on Distance to Centerline [$F(2,16) = 13.577$, $p < .001$], and the effect of Display on Vertical Velocity [$F(1,16) = 3.694$, $p = .048$]. One interaction was significant (distance from centerline; Display x Ambient Illumination x DH/RVR; $F(2,24) = 4.92$, $p = .016$). Plots of the means are shown in Figures 7, 8, 9A/B, and 10.

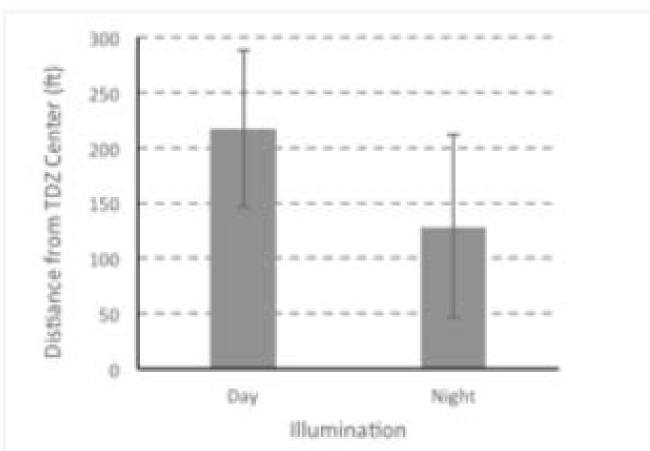

Figure 7. Mean distance from touchdown point to touchdown zone (abeam PAPI; feet) by ambient illumination.

One can see in Figure 7 that landings, on average, were a little longer during daylight conditions (216 feet beyond PAPI; contrast of runway lighting was greatly reduced) than they were in night conditions (128 feet beyond PAPI).

In Figure 8, the average distance from centerline (signed; plus values are to the right of centerline) was greatest with the HDD (9 feet), which was significantly different from the HUD without SV (2 feet) (pairwise post-hoc comparison; $p < .005$) and the HUD with SV (.04 feet) (pairwise post-hoc comparison;

p<.005), the HUD conditions not being different from one another. However, this is not a meaningful difference when one looks at the lateral dispersion of touchdown points across all trials.

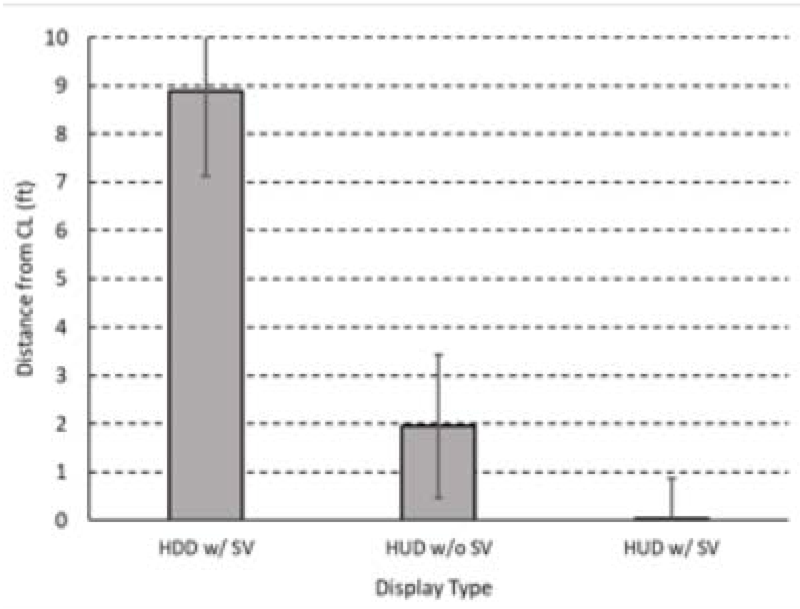

Figure 8. Mean distance from touchdown point to centerline (feet) by display type.

In Figure 9 one can see that the apparent statistical interaction is largely governed by a difference in the effect of DH/RVR within HDD and between day (A) and night (B) conditions. The other displays show the same miniscule directional differences between DH/RVR levels regardless of ambient illumination. The runway lighting was easier to see in the nighttime condition (seen sooner), but that was wholly dependent upon when the pilot chose to shift gaze out the window. In the HUD conditions, the pilot was already looking through the HUD and thus was likely able to pick up the lights the moment they appeared (usually slightly before reaching DH). That deviation was smaller at night using the HDD than it was in day conditions is also likely the result of the ease of detecting the lights at night. The difference between the two conditions in daytime for the HDD was not significant.

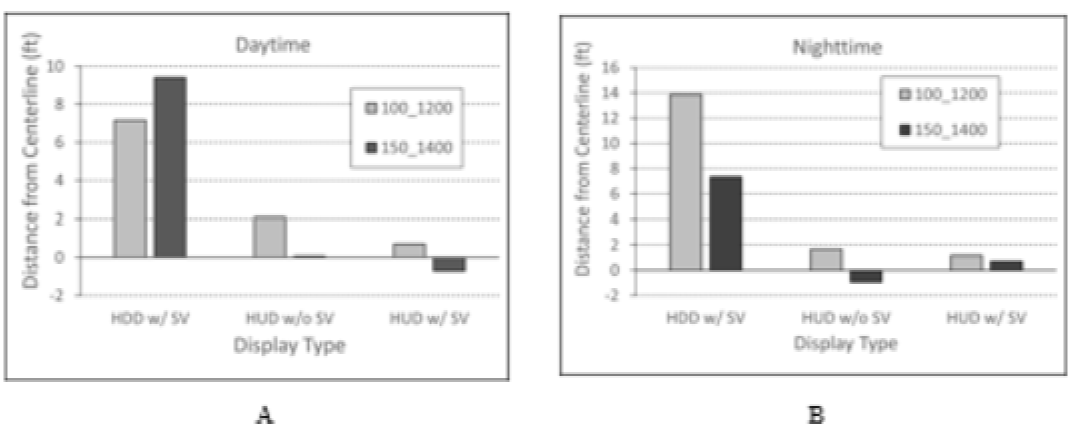

Figure 9. Three-way interaction effect on distance from centerline by Daytime (A) and Nighttime (B) ambient illumination for display type and DH/RVR.

Finally, as seen in Figure 10, the mean vertical velocity just prior to touchdown was slightly less for the HUD-without-SV condition (-3.6 fps) than either the HDD (-4.4 fps; post-hoc comparison, $p<.05$) or the HUD-with-SV condition (-4.7 fps; post-hoc comparison, $p < .05$). Vertical velocities using HDD and HUD with SV were not significantly different. Again, given the large dispersion seen among the values, these marginally significant differences would appear to have marginal operational significance. It is, however, of interest that both SV conditions had slightly higher descent rates immediately prior to runway contact than did the one display that did NOT use SV.

Variability of Means. An initial examination was conducted to determine if there was any systematic

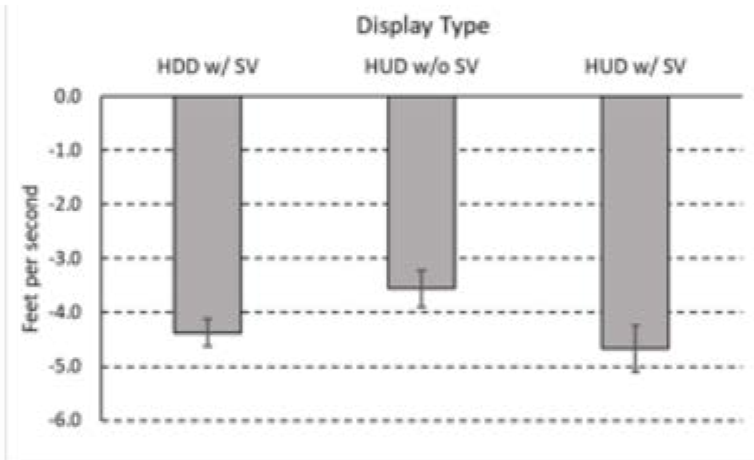

Figure 10. Mean Vertical Velocity immediately prior to touchdown by display type.

change in variability across cells as a function of any of the independent variables (IVs). This can be done by constructing an F ratio from the variances, but that would have involved a large number of post-hoc comparisons, which would have falsely inflated the experiment-wise error in the tests. A screening technique was used to determine if there were specific instances of high or low variability in any cells that should be subjected to a statistical comparison. Range widths (absolute) and the variation for each cell (to determine if outliers were influencing the central tendency and dispersion) were determined and added to an Excel spreadsheet with each cell labeled independently by the various IV levels. The rows (cells from design) were then rank ordered by increasing range width (which closely corresponded with the variation) and anywhere from 3 to 5 blocks were color coded to represent different contiguous values (ranges). The data were subsequently sorted (reordered/regrouped) by sorting on the levels of each independent variable, one IV at a time. Inspection of the resulting groupings for the variability of the mean errors indicated that there was no consistent influence, on range or variability, of any of the independent variables.

Glideslope tracking

The next analysis to be performed was able to use all of the data points because the only reason for previous exclusion was a missed approach, and that occurred after the cut-off point (threshold) for calculation error measures for glideslope (GS) and localizer (LOC) error. Figure 11 depicts a representative trial showing angular error for GS and LOC as plotted against distance from the PAPI (a.k.a. distance from touchdown zone), with the threshold, the PAPI and the point at which this approach became a missed approach. Keeping in mind that GS indications go “off the chart” as it were very close to the runway, we elected to preclude the possible inclusion of these extreme and expected excursions of the indicator from the calculation of root-mean-square error (RMSE; index of variable error). Thus we calculated the RMSE for GS and LOC starting at the IP (release of simulator) down to the threshold (vertical line in Figure 11 as referenced in the figure key) for each approach. We also used this same window for the calculation of the signed mean error (bias error index). The minimum and maximum values were also extracted from within this window to determine how far off any particular approach on either axis went during the descent.

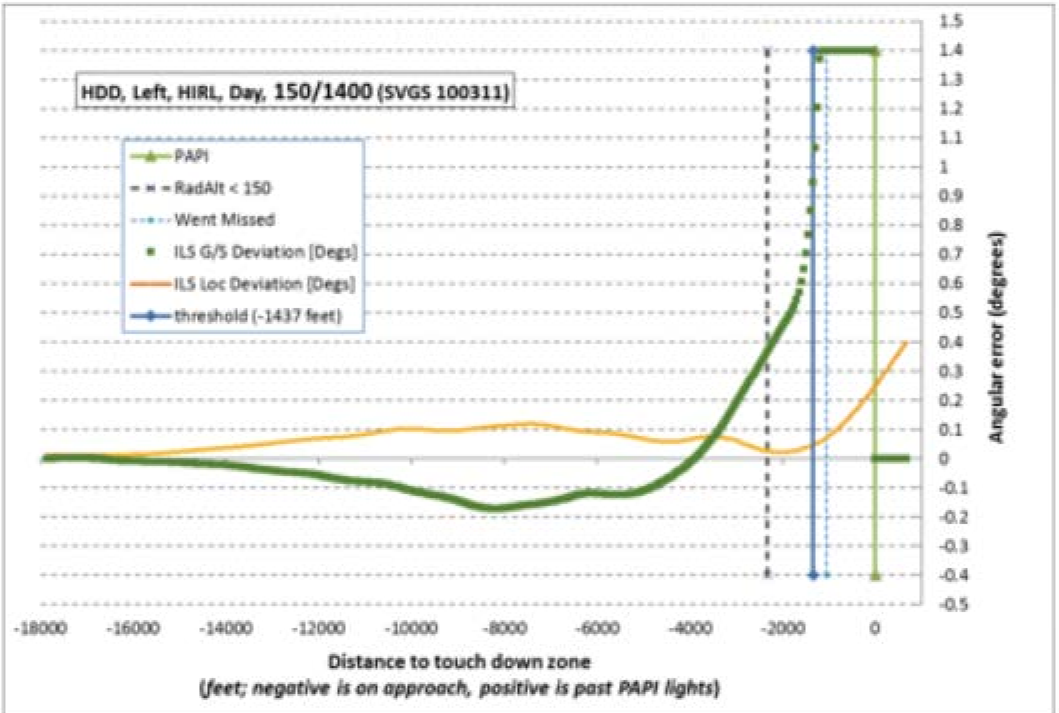

Figure 11. Representative plot of one approach to illustrate threshold cut-off for error calculations.

Glideslope RMSE (variable error). An ANOVA of the same description as previously (4-factor) was conducted on variable error (RMSE) for glideslope tracking. This analysis produced only one statistically reliable effect, and that was the influence of Display [$F(2,24) = 5.11$, $p = .014$]. The means by display are shown in Figure 12.

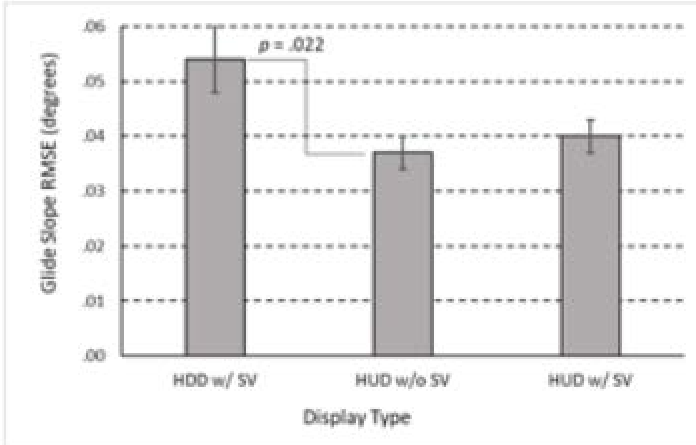

Figure 12. Main effect of display type on glideslope variable error (RMSE) and post-hoc comparison of HDD and HUD (no SV) formats.

Post-hoc comparisons indicated that only the largest mean difference attained significance (head-down display versus head-up display without SV; see Figure 12). The differences between the HUD configurations and between the conditions using SV were not significant.

Glideslope Bias (mean) error. Average glideslope bias error was calculated and analyzed using the same 4-way ANOVA configuration as employed previously. In this instance there was one main effect of Display [F(2,24) = 3.65, *p* = .041) and a significant Display by Illumination (ambient) interaction [F(2,24) = 6.265, *p* = .006]. The main effect (see Figure 13) is straightforward; approaches with the HDD were, on average, closer to unbiased high or low whereas approaches with either form of the HUD were biased

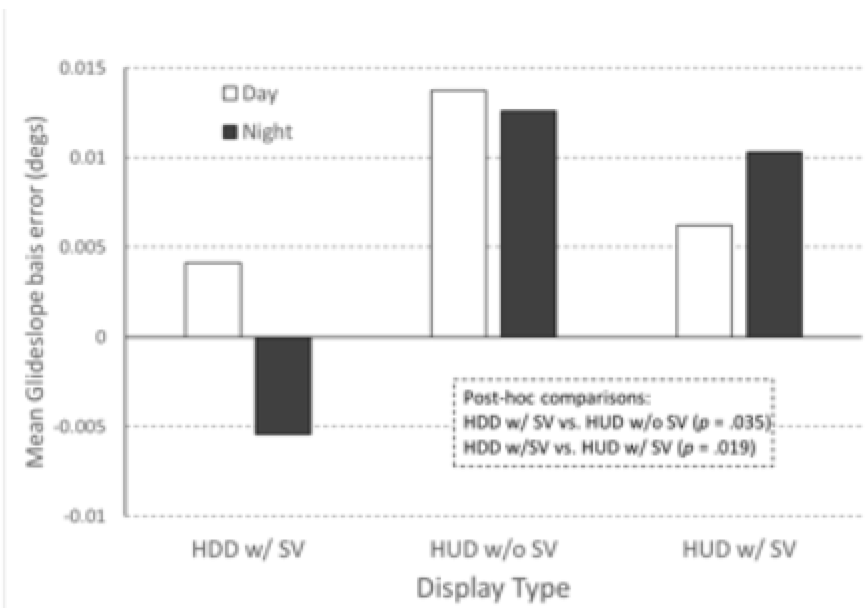

Figure 13. Mean glideslope bias error by Display and Ambient Illumination.

to be slightly low by a very small amount. The overall effect of illumination, however, was not significant for glideslope bias. These values are extremely small (the conversion for GS is .352 = 1 dot error for glideslope; LOC is .794 = 1 dot), and thus, despite being “statistically” significant, have little operational or practical significance. That is to say the approaches (tracking the localizer and the glideslope) were flown well within tolerance, on average, and there was no operationally significant bias high or low or to the left or to the right.

Localizer RMSE (variable error). Analysis of localizer RMSE indicated that the main effect of Display was significant [F(2,24) = 1.72, $p < .001$) and that the interaction of Display and Runway Lighting was significant [F(4,48) = 3.273, $p = .019$]. The means for display by runway lighting are shown in Figure 14. Upon closer inspection, it is evident that the interaction is likely largely an artifact and results from the slight inflection in the HUD-no-SV data for the middle level of lighting AND from the slight downslope (lower RMSE) with the HDD as the lighting infrastructure is increased. This is particularly notable as likely an artifact given that RMSE calculations only included values up to the runway threshold and thus there would have been very few data points used that occurred during the visual acquisition of the runway environment. Regarding the main effect post-hoc comparison, Figure 14 also shows that performance with each display was significantly different from that with every other display, and head-down display was favored with the lowest localizer RMSE.

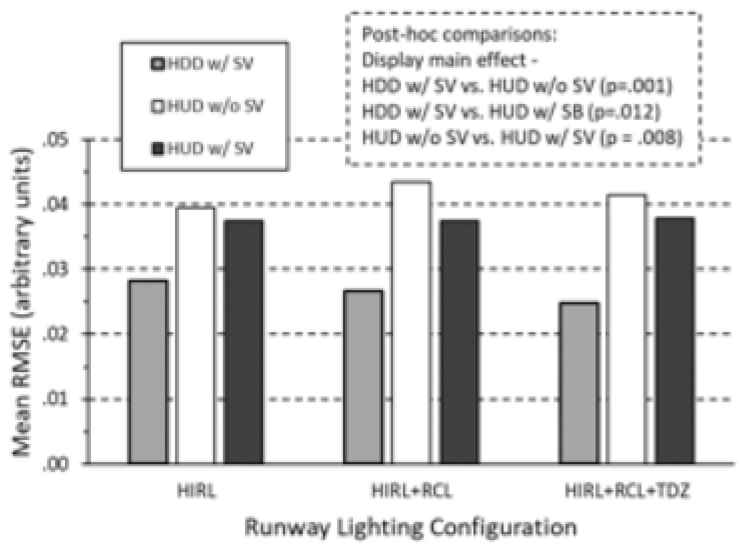

Figure 14. Mean localizer RMSE by Display and Runway Lighting Condition.

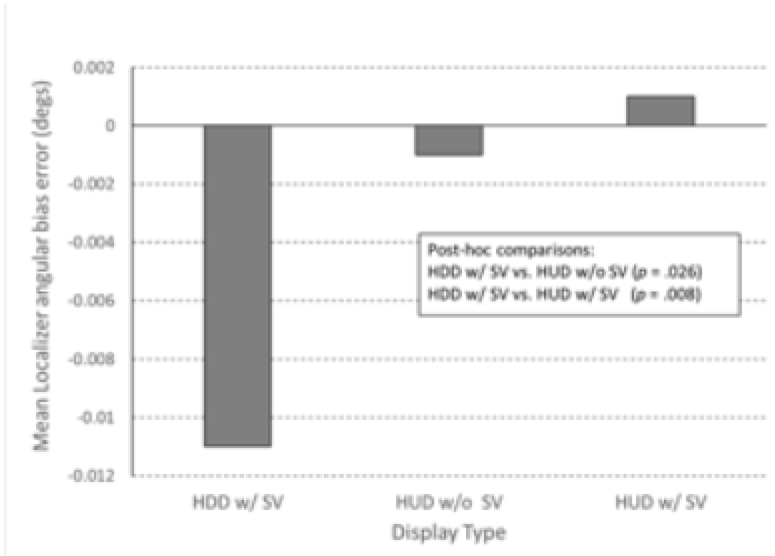

Figure 15. Mean angular bias error for localizer by display type.

Localizer bias (mean) error. The same 4-way ANOVA was conducted for localizer bias error. In this case only one main effect, that of display type, was present [F(2,24) = 7.894, p = .002]. The means are presented in Figure 15. The post-hoc comparisons indicated that bias error with the head-down display was significantly different from that with either of the head-up configurations, but that the head-up configurations did not differ from one another. Again, keeping in mind the conversion of the angular value to display dots (for LOC, .794 = 1 dot), the average bias indicated here is so small as to be inconsequential at best.

In addition to these mean errors, it is useful to know how the underlying values were distributed to have a sense of the variability/spread of the distribution. To that end, a series of box plots were developed to show the mean and the standard error (and 95% confidence interval) for the values obtained. That plot corresponding to the means presented in Figure 15 is shown in Figure 16 following. It is worthwhile noting that the variability is substantial in comparison with the difference in the means and, as such, those mean differences are inconsequential taken in context. It is also interesting to note that the head-down display, in this case, was associated with the *least variation* in performance.

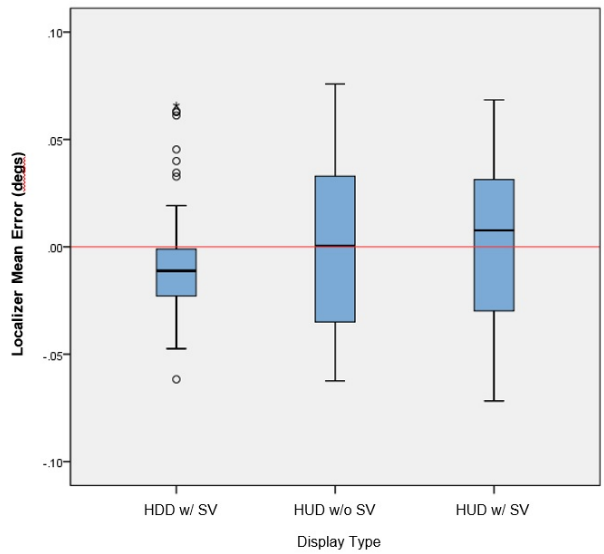

Figure 16. Box plat representation of means in Figure 15 with standard deviations and 95% confidence interval.

Acquisition of Runway Environment

The pilot flying was required, as part of the task, to verbally call out "field in sight," "runway," or whichever verbalization his company used in normal operations. In some cases, this was "lights" to signify seeing the approach or runway lights. We used this metric in lieu of more complicated procedures (i.e., eye tracking, which would indicate where they were looking but not what they were seeing necessarily) to assess when the pilot thought he had acquired the runway. Due to a problem with the RadAlt measure involving significant variations in terrain height leading up to and immediately before the runway threshold, we opted to use altitude MSL as the dependent measure. As one would expect, the same trials in which we did not have a touchdown point due to a go around were the same trials in which we did not have a call of the runway. As such, the same data were thus excluded from the analysis as were excluded in that prior analysis.

Only two main effects were found to have significant effects on the point at which the runway or its immediate environment was visually acquired, Display [$F(2,14) = 8.328$, $p < .005$] and DH/RVR [$F(1,7) = 25.835$, $p = .001$). The two effects are shown following in Figures 17A and 17B. Post-hoc comparisons for Display indicated that the acquisition altitude was higher for the HUD no SV (470 feet MSL) than HDD (452 feet) (post-hoc comparison, p<.01), and was greater than with the HUD with SV (459 feet) (post-hoc comparison, $p < .05$). The difference between HUD and HUD with SV was not significant, that mean difference being only 11 feet or so. Taken in context, the largest significant difference of 19 feet does not appear to be operationally significant. The altitude MSL at which the runway was acquired was significantly higher, statistically, when RVR was 1400 (471 feet) than when it was 1200 (449 feet), a mean difference of 22 feet.

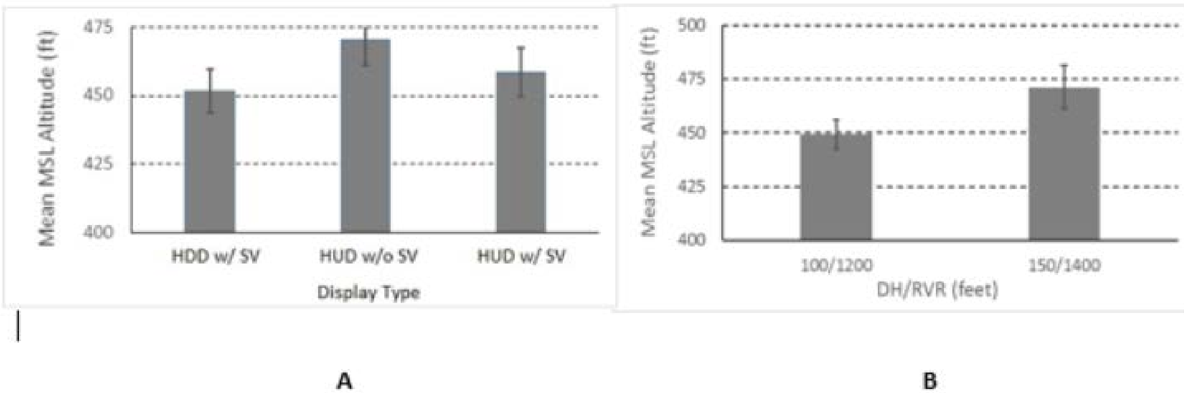

Figure 17. Effect of Display (A) and of DH/RVR (B) on altitude MSL at which runway was visually acquired.

It should be noted here that there were significant issues that arose related to the selection and use of this particular approach on this particular runway that impacted some of the data analyses. One thing that directly affected pilot ability to discern between the RadAlt indications for a DH of 150 and one of 100 feet was the sloping terrain immediately before the approach end of the runway. There the terrain is significantly below the runway and thus the RadAlt indication increases suddenly upon starting to cross the ravine on approach and then goes down again suddenly on the upslope to the runway. Table 2 presents data describing this relationship quantitatively by time along the approach (simulator time) and the various altitude metrics.

Table 3. Values on approach for three altitude measurements by elapsed time just before runway.

Sim time (secs)	Alt. above threshold (ft)	RadAlt reading (ft)	Alt MSL (ft)
61.592	95	162	450
61.792	93	124	448
61.992	91	97	446

The difficulty for the pilot was that the RadAlt indication (changing in 5-foot increments on the PFD) went from just over 150 to under 150 and then under 100 within the space of a second. This was confirmed on the video record (showing RadAlt instrumentation in the cockpit) going from 200 to 190, then a flicker, then 135, then 90 all very quickly in confirmation of what the digital data record showed. Thus, it is difficult if not impossible to say anything about the DH component of this independent variable because it appears that the pilots were not given sufficient time to discern between and respond to an indication of 150 versus an indication of 100. Thus little can be said relative to the DH assignment for these conditions, and virtually all of the effect and subsequent discussion must therefore center about the

RVR portion of the combination (1400 or 1200). Thus, further discussion will treat any effects related to this variable as related to the visibility only.

Go-arounds

Of the 507 approaches performed by the participants, only 7 of them (1.38%) resulted in a go-around. Examination of the distribution of these events indicated that one individual was responsible for 43% of all go-arounds, another was responsible for 29%, and two other individuals had one each (14% each). These were also distributed such that all occurred when using the HDD, 86% occurred in daytime conditions (reduced contrast of runway lighting), 3 with minimum runway lighting, and two with intermediate runway lighting. Thus, this extremely small number of events was linked to the most challenging conditions and to a small number of individuals. It was noted through real-time observation by the test monitors that the individual responsible for 3 go-arounds wore glasses, seated himself a little bit low, and was a bit slumped over when using the HDD. This placed his head in a position where he was not able to see adequately over the glare shield and acquire the runway consistently in the lower-visibility conditions although we, as observers, were able to see that the runway or lights were visible in the out-the-window view. A summary of these events by conditions is presented in Table 4.

Table 4. Go-arounds by crew/captain and independent variable levels.

Crew (Capt.)	**Display**	Runway Lights	**Ambient Ill.**	DH/RVR
2	**HDD w/ SV**	HIRL/RCL (1)	**Day**	150/1400
2	**HDD w/ SV**	HIRL/RCL/TDZ (2)	**Day**	100/1200
3	**HDD w/ SV**	HIRL (0)	**Day**	150/1400
10	**HDD w/ SV**	HIRL (0)	**Day**	150/1400
10	**HDD w/ SV**	HIRL (0)	Night	100/1200
10	**HDD w/ SV**	HIRL/RCL (1)	**Day**	100/1200
12	**HDD w/ SV**	HIRL/RCL/TDZ (2)	**Day**	150/1400

Practice trials

The total number of practice trials varied considerably from one captain to another. Recall that the FO was not a determiner of exit from practice/training in any way and did not contribute to the flying performance of the aircraft. Thus, use of the term "crew" in virtually all cases implies the performance of the pilot flying. As such, the total number of trials ranged from 3 to 10 (mean = 6.15 trials; mode = 6). A plot by crew is shown in Figure 18. If one looks at the average number of trials by display type, the values are HUD without SV, 1.08; HUD with SV, 2.3; HDD, 2.77. Using F for paired comparisons, HUD without SV required significantly fewer trials than either of the other formats (versus HUD SV, $p < .0001$; versus HDD, $p < .00001$; number of trials between the two SV-depicting displays did not differ significantly). This is not surprising inasmuch as the HUD without SV is the standard display on which the captains had to be qualified to be able to participate in the study. Both of the other displays contained novel content to which the participants needed to adjust, and thus a larger number of trials was needed.

Posttest Interview/Questionnaire

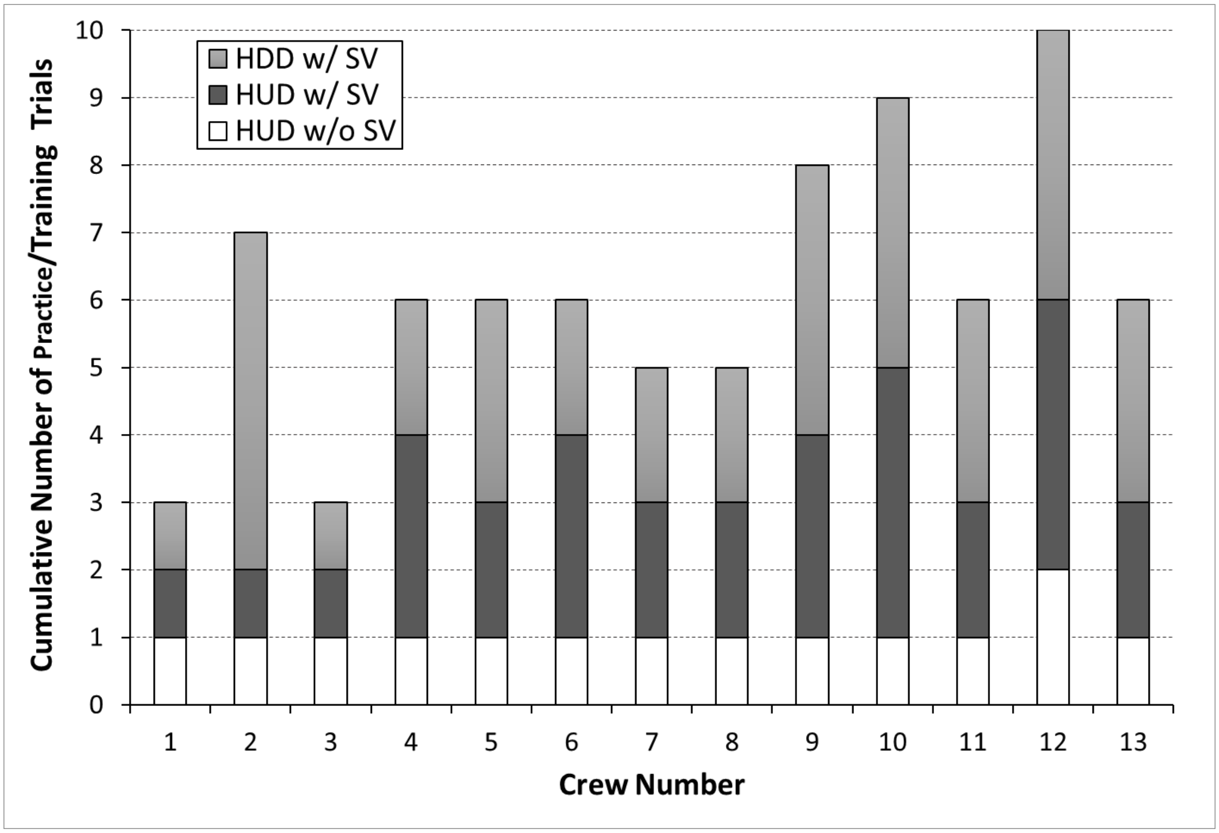

Figure 18. Cumulative number of training trials by display type and crew number.

Preference for training type. It is appropriate, at this point, to bring in the data from the posttest interview and begin with an item that was related to training to connect their simulator training with their training preferences. When the pilots flying were asked to rank their preferences for the type of training they would prefer for the SV-portraying display platforms, they ranked training in a flight simulator as the first preference, and handbook training was ranked last. Video and CBI were favored, approximately equally, over classroom or internet-based training, and those 4 fell between the other two. These rankings, showing the mean, median, and mode for each, are depicted in Figure 19. In this figure, the ranks are reversed for graphing effect, so that 6 = most preferred (first) and 1 = least preferred (last).

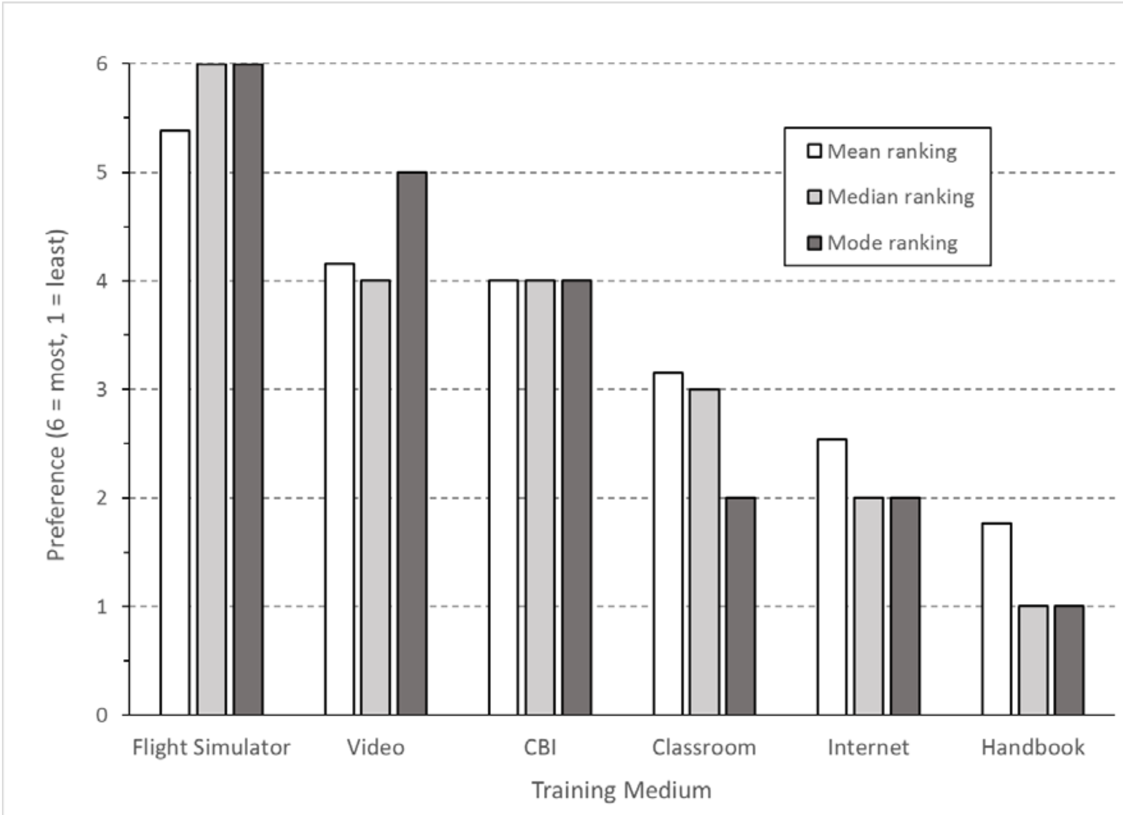

Figure 19. Rank-ordered preference by possible SVGS training medium.

Acceptable minima by equipment type. Another question of interest was to what minima the pilot would be willing to fly as a function of the equipment installed in the aircraft. Figure 20 shows this relationship between equipage and the point in the DH/RVR space where pilots believed they could operate as a result. Although the results were not as spaced between equipment options as those found with GA pilots (Beringer, 2016), they were in the expected direction of “more” equipment equals lower minima. It was not surprising that the two HUD configurations clustered together to provide the lowest minima to which pilots would be willing to fly, and also that adding SV to the head-down PFD also decreased the minima to which pilots believed they could/would fly.

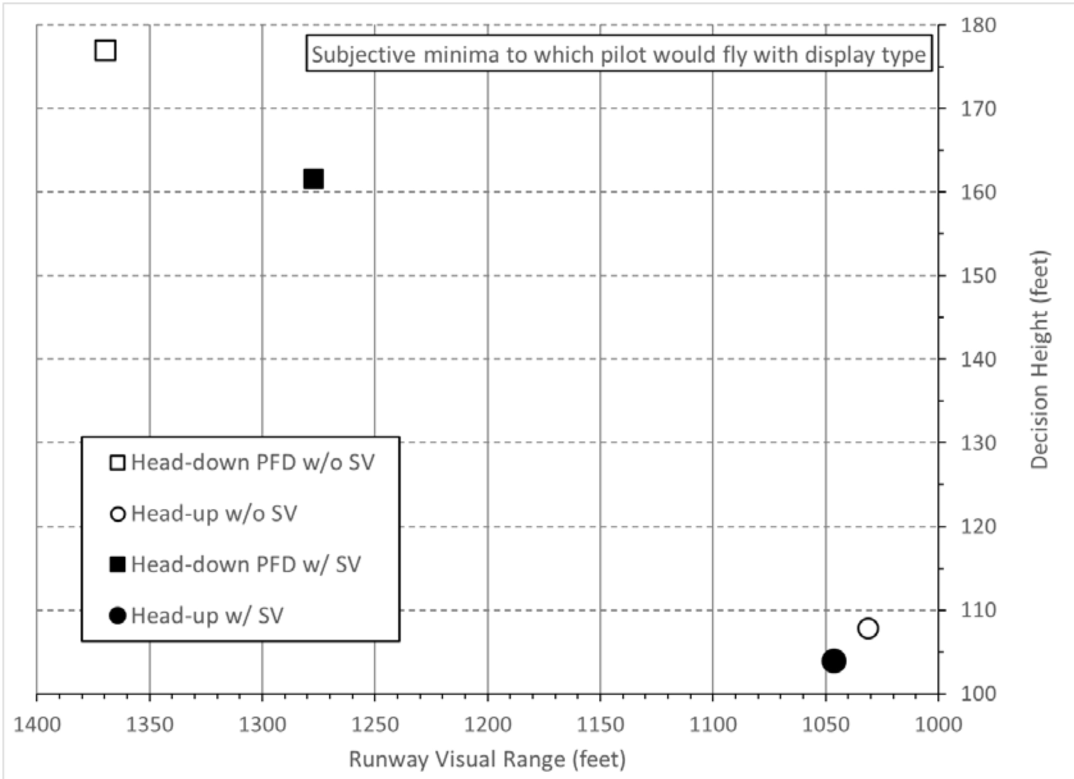

Figure 20. Average subjectively expressed minima combinations to which pilots believed they would be willing to fly as a function of installed display equipment.

Self-rating of acceptability of touchdowns. Pilots were asked, posttest, how they rated their touchdowns on a scale of not acceptable to acceptable as a function of the display type used. Figure 21 illustrates the distribution of these responses. Pilots perceived that their touchdowns were more acceptable when using one of the HUD configurations than when using the head-down configuration. Note that the graph is scaled to allow both extraction of the actual number of responses per display type and category (out of 13 possible) but also a sense of what percentage that represents as a function of the height of the bars (top of the Y axis would be 100%). Inasmuch as there was a great deal of adaptation taking place during these trials (no previous experience with the head-down configuration and a significant history using HUDs), this perception is not unexpected. One of the frequent comments made, posttest, by the pilots was that they believed they could do much better with the head-down format if (1) they had more practice/training using it and (2) if some of the graphical representations on the head-down display were modified to be more consistent with their (participants') expectations. Note that five respondents did rate their touchdowns as very acceptable or sufficiently acceptable with the head-down display.

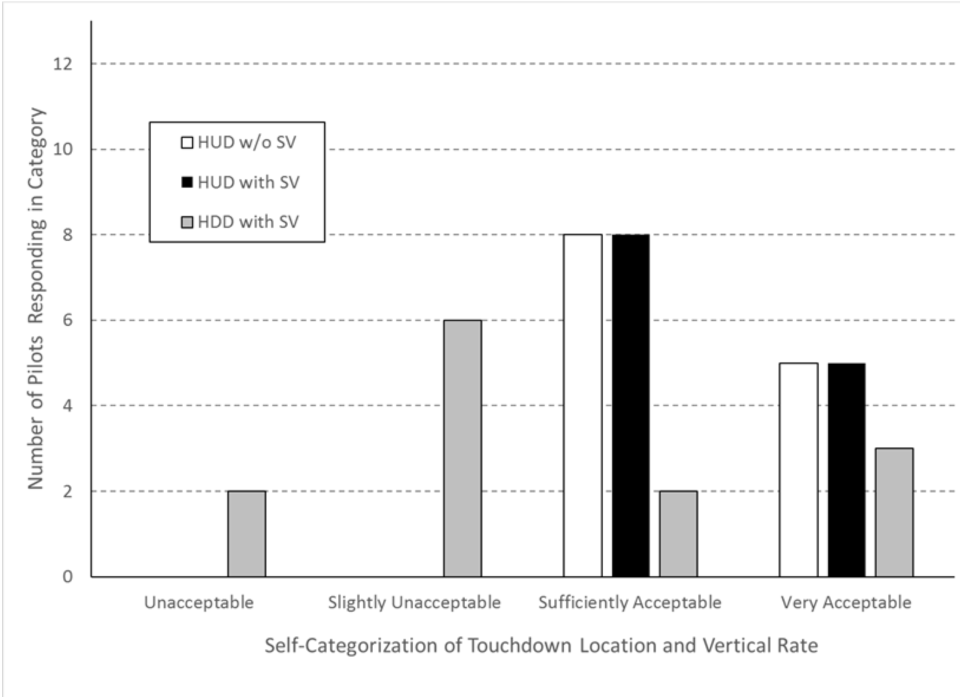

Figure 21. Pilot self-rating of acceptability of touchdowns by display type used.

Perceived Workload. Participants were also asked to subjectively rank-order the three displays according to highest/lowest perceived levels of workload. Those results are shown in Figure 20. While it was not surprising that the majority subjectively rated the head-down display as involving the highest workload, there were two other pilots who placed it in the other two categories, one even placing it in the lowest-workload category**.** It was to some degree surprising that the HUD with SV was equally frequently considered to impose the LEAST workload, in the participants' opinion, and that the conventional HUD (no SV) placed most frequently in the "middle" category. Participants were also asked, in a parallel question, to state their rank ordering of preference for display type. The distribution very closely mimicked that in Figure 22, so those data will not be reported herein.

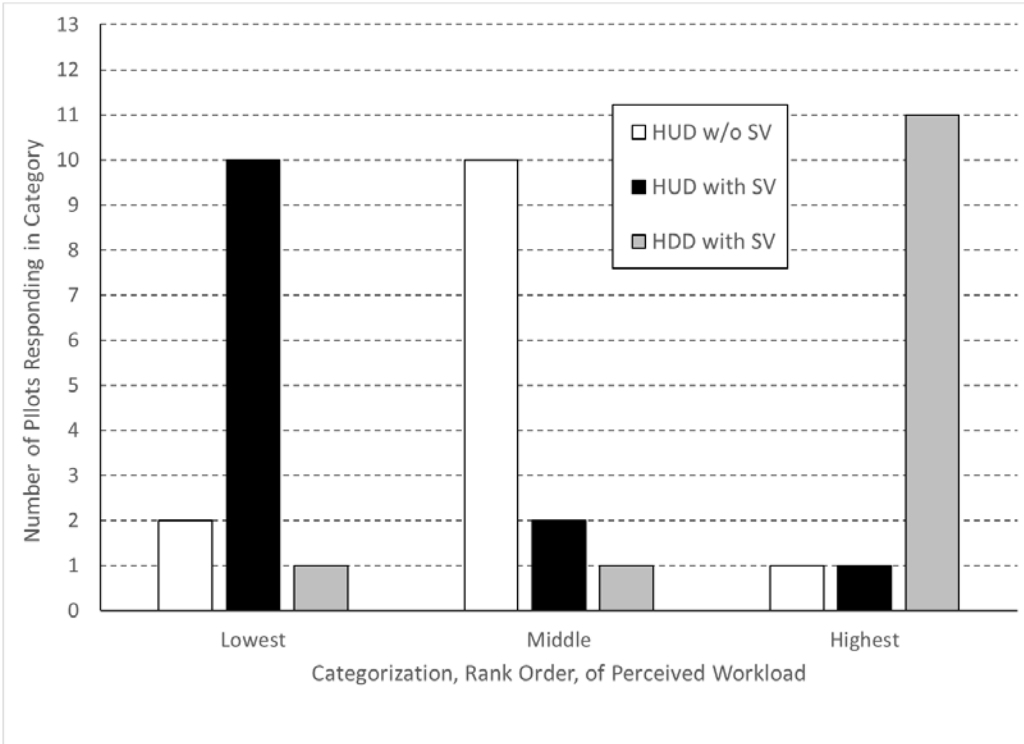

Figure 22. Distribution of responses to rank ordering of display type by perceived workload.

Contribution to stable approach. Participants were asked to rate to what degree they believed the presence of synthetic vision on the displays contributed to stability of the approach. It is apparent that the general opinion, as seen in Figure 23, was that it did make a positive contribution to some extent, with most responses being in the "significantly," and "a reasonable amount" categories. Synthetic vision on the HUD was seen as contributing more in the "significantly" category, whereas the head-down version was more often placed in the "a reasonable amount" category.

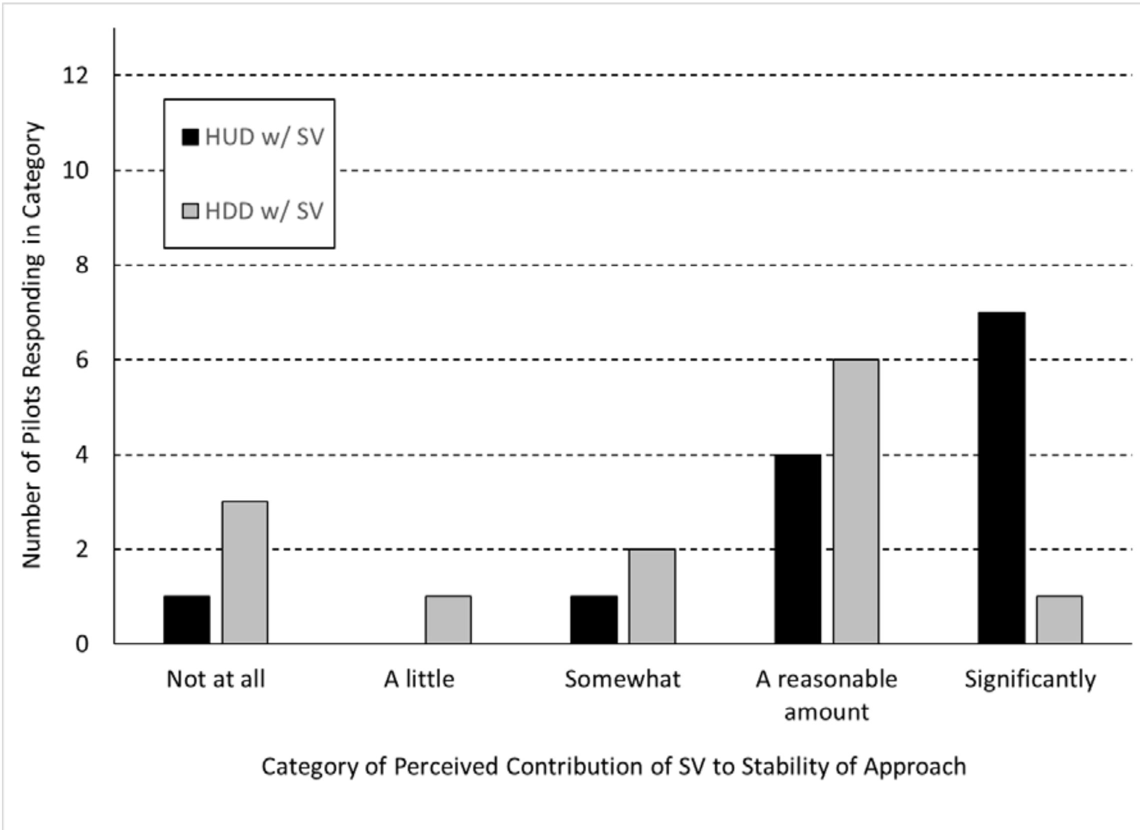

Figure 23. Perceived degree to which the SV-depicting display contributed to a stable approach.

Stated uses of synthetic vision during the approach. Pilots were asked both what types of uses they found for the synthetic-vision imagery when flying the approaches. All of them mention, first, (1) general situational awareness, with the majority also mentioning (2) confirming location on the approach and (3) confirming the position/location of the runway upon reaching DH. When asked how often they viewed three of the features on the display, those being terrain, the runway image, and the flight-path marker, the flight-path marker was viewed either "continuously" or "frequently." The runway image was characterized the same way. The terrain, however, was seen as being viewed much less frequently.

There were additional "opinion" questions posed to the participants, but the responses were either deemed undiagnostic regarding a differentiation between the displays or the questions themselves were regarded to have not been adequately couched or to call upon a pilot evaluation that was too subjective and unquantifiable. As such, the remainder of the interview/questionnaire results are not included herein.

CONCLUSIONS

Taken as a whole, the data suggest that there were no performance differences between approaches using the head-down and the head-up synthetic-vision displays that appear to rise to the level of significant operational consequence. That the pilots expressed a preference for the head-up format and for some modifications to both SV depictions was not surprising, particularly given that the head-down display had to be presented in a somewhat compromised format, using the existing PFD display hardware in the 737 simulator. This display was small and square as compared with the sizes and wide aspect ratios of some of the head-down PFDs that are being marketed today. Thus, one could expect that performance could improve and complaints be reduced by implementing the head-down PFD on display hardware consistent with current-generation avionics that host SV. It is also worth noting that, once again, we have seen a dissociation between pilot preference and pilot performance wherein pilots have a preference for something but performance indicates that pilots are able to perform adequately using a lesser-preferred system.

It is also worth noting that there was considerable variation in the crews' responses to the head-down display. Some liked it a great deal while others were put off by it, the latter largely being the older pilots with a significant amount of HUD time/experience and no experience with head-down electronic PFDs hosting Synthetic Vision. It is, however, worth keeping in mind that some differences between pilot performances, by display type, were observed under the worst conditions in which to acquire the airport infrastructure visually; minimal airport infrastructure and daylight ambient illumination (higher, but extremely small, likelihood of a go-around). It should be noted that other performance measures did not mirror this, and the incidence of occurrence was extremely small. In summary, it appears that the head-down PFD format depicting synthetic vision cues is capable of supporting low-visibility approaches, even in cases where there may be reduced lighting infrastructure. It is recommended that some additional evaluation may be warranted using a contemporary-design wide-format PFD that is optimized for pilot adjustability, brightness/contrast, clutter reduction, and other factors that have been demonstrated to influence both pilot performance with and pilot perception of displays.

ACKNOWLEDGMENTS

Research reported in this paper was conducted under the Flight Deck Program Directive/Level of Effort Agreement between the Federal Aviation Administration Human Factors Division (ANG-C1) and the Aerospace Human Factors Research Division (AAM-500) of the Civil Aerospace Medical Institute. The authors would like to thank a number of individuals who participated in the preparation for and conduct of this study and in the reduction and analysis of the data. These include: Flight Operations Simulation Branch - Randall Cooper, Larry Miller, Douglas Rodzon, Vincent Liao, Peter Rohde; Zedasoft – Rob Hatcherson, Victor Shortt; Cherokee CRC, LLC – Joey Jaworski, Suzanne Thomas, Ester Devaney, Shijing Liu, Dan Jack, Hunter Klevgard, Janine King; Sponsors (Flight Operations Branch) - Janet Greenwood, Terry King, Chris Hope.

REFERENCES

Beringer, D. B. (2016). An exploratory evaluation of general aviation pilot performance and preferences using synthetic vision displays for approaches and missed approaches in flat and challenging terrain. Proceedings of the Human Factors and Ergonomics Society Annual Meeting. (pp. 76-80)

Brown, A. D. (1970). Category II - A simulation study of approaches and landings at night. Royal Aircraft Establishment, Technical Memo Avionics59 (BLEU), England.

Calvert, E. S. and Sparke, J. W. (1958). The effect on weather minima of approach speed, cockpit cutoff angle and type of approach coupler for a given landing success rate and level of safety. Aeronautical Research Council Technical Report. C.P. No. 378.

Ellis, K. K. E., Kramer, L. J., Shelton, K. J., Arthur III, J. J., & Prinzel III, L. J. (2011). Transition of attention in terminal area Nextgen operations using synthetic vision systems. Human Factors and Ergonomics Society. Proceedings of the Human Factors and Ergonomics Society 55th Annual Meeting; (46-50).

Ellis, K. K. E., Arthur III, J. J., Latorella, K. A., Shelton, K. J., Norman, R. M., & Prinzel III, L. J. (2012). Quantifying pilot visual attention in low visibility terminal operations. 4th AHFE International Conf. on Applied Human Factors and Ergonomics 2012; July 20-25 2012; San Francisco, CA; National Aeronautics and Space Administration, Langley Research Center, Hampton, VA.

Eversmeyer, L., Reisweber, M., Liao, V., & Avery, S. (2008). Human-in-the-loop pilot demonstration category I instrument landing system approaches to 200’ decision height and 1800 RVR minima and CAT II approaches on type I ILS to 1600 and 1200 RVR. DOT-FAA-AFS-440-40, Federal Aviation Administration, Oklahoma City, OK, March.

FAA (2017). FAA Historical Chronology, 1926 – 1996. Federal Aviation Administration. Retrieved from https://www.faa.gov/about/media/b-chron.pdf.

FAA (2009). Procedures for the Evaluation and Approval of Facilities for Special Authorization Category I Operations and All Category II and III Operations. FAA Order 8400.13D, October 22.

FAA (2010). Visual Guidance Lighting Systems. FAA Order 6850.2B, 20 August.

Garbell, M. A. (1951). Recent developments in visual low-approach and landing aids for aircraft. Illuminating Engineering, 46(7), 353-8.

Haines, R. F. (1980a). Head-up transition behavior of pilots during simulated low-visibility approaches. NASA Technical Paper 1618. National Aeronautics and Space Administration, Ames Research Center, Moffet Field, California, June, 1980.

Haines, R. F., Fischer. E., & Price, T. A. (1980b). Head-up transition behavior of pilots with and without head-up display during simulated low-visibility approaches. NASA Technical Paper 1720. National Aeronautics and Space Administration, Ames Research Center, Moffet Field, California, December.

ICAO (2013). Aerodrome Design and Operations. Annex 14 Aerodromes, Volume 1, 6th Edition, International Civil Aviation Organization, July.

Korn, B. R., Lenz, H., & Biella, M. (2007). EVS: head-up or head-down. American Institute for Aeronautics and Astronautics. 26th Digital Avionics Systems Conference. Oct. (5.A.3-1 – 5.A.3-9).

Korn, B. R., Biella, M., & Lenz, H. (2008). Operational landing credit with EVS head down display: Crew procedure and human factors evaluation. Proc. SPIE Volume 6957 69570K-1. Enhanced and Synthetic Vision 2008, Guell, J. J. and Uijt de Haag, M. eds.

Kramer, L. J., Williams, S. P., & Bailey, R. E. (2008). Simulation evaluation of synthetic vision as an enabling technology for equivalent visual operations. Proc. SPIE Volume 6957, 69570K-1. Enhanced and Synthetic Vision 2008, Guell, J. J. and Uijt de Haag, M. eds.

Kramer, L. J., Bailey, R. E., Ellis, K. K. E., Norman, R. M., Williams, S. P., Arthur III, J. J., Shelton, K. J., & Prinzel III, L. J. (2011). Enhanced and synthetic vision for terminal maneuvering area nextgen operations" Proc. SPIE Volume 8042, 80420T, Enhanced and Synthetic Vision 2011, Guell, J. J., Bernier, K. L., Thomas, J. T., & Desjardins, D. D. eds.

Kramer, L. J., Bailey, R. E., Ellis, K. K. E., Williams, S. P., Arthur III, J. J., Prinzel III, L. J., & Shelton, K. J. (2013). Enhanced flight vision systems and synthetic vision systems for next gen approach and landing operations. National Aeronautics and Space Administration. Langley Research Center. NASA/TP–2013-218054, Langley, Virginia. November.

Lybrand, W. A., Vaughan Jr., W. S., & Robinson, J. P. (1959). Airport marking and lighting: operational tests and human factors. Appendix X, selected annotations and bibliography. Human Sciences Research, Inc. AD-756677, NTIS, May.

RTCA (2015). Minimum Aviation System Performance Standards (MASPS) for Synthetic Vision Guidance Systems, DO-359, RTCA, Washington, DC., May 18.

Spady, A. A. (1978). Airline pilot scan patterns during simulated ILS approaches. NASA Technical Paper 1250. National Aeronautics and Space Administration, Langley. Virginia, October.

Swartz, W.F., Condra, D.M. and Madero, R.P. (1976). Pilot factors considerations in see-to-land. Technical Report AFFDL-76-52. Air Force Systems Command, Wright-Patterson Air Force Base, Dayton, Ohio. May.

14 C.F.R. § 91.176 (2017). Straight-in landing operations below DA/DH or MDA using an enhanced flight vision system (EFVS) under IFR. Retrieved from (http://rgl.faa.gov/Regulatory_and_Guidance_Library/rgFAR.nsf/0/AB762DDDCE26CBC186258106007680CE?OpenDocument)

Appendix A: Pilot Experience Assessment

Pilot Experience Assessment

Crew # ______________________ Date: _______________________

1) Pilot participating as: ❑ Pilot Flying ❑ Pilot Monitoring

2) What ratings do you hold currently?

- ❑ Airline Transport Pilot (ATP)
- ❑ Certified Flight Instructor (CFI)
- ❑ Certified Flight Instructor – Instrument (CFII)
- ❑ Other __________________

3) Current flight crew position: ❍ Captain ❍ First Officer

4) Year that you began licensed flying: _________

5) Present age: __________

6) Sex (M/F) ____________

7) Please estimate your flying hours

Category of Hours	**Total in category**	**Last 90 days**	**Last 30 days**
*Actual **IFR***			
*Simulated **IFR** in aircraft*			
Flight simulator time			
All flight hours			

8) Are there any restrictions on your medical certificate? If so, please identify below -

(i.e., holder shall wear correcting lenses, etc.)

9) What was the approximate date (month/year) of your last proficiency check? ____/____

10) Have you used an enhanced flight vision system (EFVS) on a Heads-Up Display (HUD) in actual operations? ❍ Yes ❍ No

If you answered yes, please answer the following questions:

a) Approximate date of last use: __________

b) Approximately how many approaches have you flown while using EFVS? ________

i. Make or model of display/system if known ____________________

ii. Type of aircraft in which installed ________________

11) Have you used a Synthetic Vision System (SVS) displayed on a head down display during actual operations? ❍ Yes ❍ No

If you answered yes, please answer the following questions:

a) Approximate date of last use: __________

b) Approximately how many approaches have you flown while using SVS head-down displays? ________

i. Make or model of display/system if known ____________________

ii. Type of aircraft in which installed ________________

Also if you answered yes, please indicate, specifically, if you have flown any of the following display systems with the Synthetic Vision (terrain depiction) option installed:

a) Chelton (now known as Cobham Systems) PFD/MFD yes / no

b) Garmin: G 420 G 430 G 530 GTN 650 GTN 750

G 600 PFD G 1000 G 2000 G 5000 (please circle each used)

c) Aspen or Avidyne avionics or other after-market retrofit electronic displays Yes / No (Please list any other display systems that you have experience flying)

d) Any Rockwell or Honeywell systems with Synthetic Vision Yes / No

Appendix B: Structured Post-test Interviews

Post-test Interview, Pilot Flying, SVGS

1) To what degree did you feel that having the Synthetic Vision imagery did or did not contribute to the stability of the approach? (please circle your responses, one for each)

a) On the HUD: Not at all A little Somewhat A reasonable amount Significantly

b) On the HUD: Not at all A little Somewhat A reasonable amount Significantly

2) How frequently did you refer to each of the various SVGS display features (terrain, runway, FPV)? (circle one for each item)

a) Terrain: Not at all Infrequently < 50% > 50% Frequently Continuously

b) Runway: Not at all Infrequently < 50% > 50% Frequently Continuously

c) Flight-path Marker: Not at all Infrequently < 50% > 50% Frequently Continuously

3) How did you use the SVGS on the approach? If you used it for more than one purpose, put a number in the parentheses following the item to show how much; 1 for most, 2 for second most, etc.

a) general situational awareness ( )

b) confirm location/position on the approach ( )

c) confirm position relative to the runway at/near DH and at transition ( )

d) Other (list):

4) How acceptable, to you, were your touchdowns (e.g. alignment with centerline, distance from planned touchdown point, sink rate at touchdown)?

a) For standard HUD without SV:

Unacceptable Slightly unacceptable Sufficiently acceptable Very acceptable

b) For HUD with SV:

Unacceptable Slightly unacceptable Sufficiently acceptable Very acceptable

c) For HDD with Synthetic Vision:

Unacceptable Slightly unacceptable Sufficiently acceptable Very acceptable

5) Please rank the three display types (HUD/no SV, HUD/with SV, HDD with SV) in order of your preference for flying this type of approach. (1 for most preferred; 3 for least preferred).

( ) Head-down display with SV ( ) Standard HUD ( ) Head-Up Display with SV

Please include a brief explanation of your ranking, especially for the most and least preferred:

6) Please rank the three display types based on your perceived workload during the approach. (1 for least perceived workload; 3 for highest perceived workload)

( ) Standard HUD (no SV) ( ) Head-Down Display with SV ( ) HUD with SV

Please include a brief explanation of your ranking, especially for highest and lowest workload:

7) For the HUD-with-SV trials, did the SVGS imagery, at any point, obscure the OTW view to the degree that it interfered with your forward view of the runway? (yes / no)

As a corollary to the above question and depending upon your response above:

8) What would you want as an option at break-out when acquiring the runway using the head-up display?

(circle a, b, c or write in another option):

a. Be able to turn off the Synthetic Vision (terrain/runway) imagery in the HUD

b. Be able to dim the Synthetic Vision imagery but leave it on

c. Have the Synthetic Vision imagery remain at its normal brightness

d. Other: ____

8) Did the SVGS displayed runway contribute to earlier detection/acquisition of the landing runway when transitioning to out-the-window visual cues, which is to say, did it aid your visual search for the runway/lights?

a) HUD with SV (yes / no)

b) Head-Down Display (yes / no)

The following questions pertain to your use of display features in the simulator and to your willingness to perform approaches with and without these features in a real aircraft. Please use the labeled scales to circle a response that applies to each statement in this section.

9) I would be comfortable flying under the RVR and DH conditions presented in the approaches with the head-down display (HDD) without the terrain being shown (but with runway image).

Strongly Disagree	Somewhat Disagree	Neutral	Somewhat Agree	Strongly Agree

10) I would fly to a DH of 100 feet AGL only if the terrain (and runway) was shown on the display(s).

Strongly Disagree	Somewhat Disagree	Neutral	Somewhat Agree	Strongly Agree

11) What is the lowest DH and RVR that you would be willing to accept for each of the following equipage conditions? (select one DH and one RVR for each display configuration)

a. Head-down PFD without synthetic vision imagery
DH: 250 200 150 100

RVR: 1400 1200 1000

b. Head-up display without Synthetic Vision imagery
DH: 250 200 150 100

RVR: 1400 1200 1000

c. Head-down PFD with Synthetic Vision imagery.
DH: 250 200 150 100

RVR: 1400 1200 1000

d. Head-up display with Synthetic Vision imagery.
DH: 250 200 150 100

RVR: 1400 1200 1000

12) Please list up to 4 functions, options, or features of the SVGS that you found to be the most useful and indicate why you considered them useful.

a) ____________________

b) ____________________

c) ____________________

d) ____________________

13) Please list up to 4 functions, options, or features of the SVGS that you found to be of little or no value or to be distracting.

a) ____________________

b) ____________________

c) ____________________

d) ____________________

14) If there are features or functions that are NOT available on the SVGS you USED but that you would like to see implemented, please list them below.

15) Brightness/contrast: Please mark on the scale where you felt that each of these factors was, for you, for each of the two factors on the head-up display regarding the synthetic-vision imagery.

a. Brightness - too dim……………just right…………….too bright

1 2 3 4 5

b. Contrast - faded into …...............ok………… obscured OTW
out-the-window

1 2 3 4 5

16) Training: What training forms would you want to see for SVG systems? Please rank order the following from 1 (most desired) to 6 (least desired)

Handbook (paper or electronic)	
Computer-based instruction	
Internet (on web site)	
Video (tape or DVD)	
Classroom	
Hands-on in flight simulator	

17) Are there any operations that you believe you could perform with the SVGS that would not have been possible or easily accomplished without it?

18) Given your experience with the Synthetic Vision imagery in the two displays you used (Head-down Primary Flight Display and Head-up Display), please rate the synthetic terrain picture and flight-path marker in each for perceived overall reliability/accuracy, visibility, and possible contributions to safety on the following scales:

Synthetic Vision – the head-down Primary Flight Display synthetic terrain picture (textured full-color image)

	Poor	Below average	Above average	Excellent
Reliability/accuracy				
Visibility				
Safety contribution				

Synthetic Vision – the head-up display synthetic terrain picture (monochrome/green image)

	Poor	Below average	Above average	Excellent
Reliability/accuracy				
Visibility				
Safety contribution				

Flight-path marker on head-down Primary Flight Display – flight guidance

	Poor	Below average	Above average	Excellent
Reliability/accuracy				
Visibility				
Safety contribution				

If you placed any ratings in the “Poor” or “Excellent” categories, please expand on which feature was responsible for that rating and why you rated it that way. Your explanation is crucial to our understanding the actual way in which pilots use these systems. How you use these systems will translate directly into how the FAA’s flight test evaluates future SVS systems.

Thank you for responding to these questions. The results will be made available to participants when all forms are completed and the results tabulated.

Post-test Interview, Pilot Not Flying, SVGS

1) Did the use of Synthetic-vision displays by the pilot flying have any effect on your workload as compared with PF's use of the "standard" HUD?

Greatly Decreased	Somewhat Decreased	No Change	Somewhat Increased	Greatly Increased

2) Did the use of the synthetic-vision displays by the pilot flying have any influence on your perception of how likely you were, as a crew, to successfully complete the approach in the reduced visibilities encountered? (yes / no) (If yes, enter comments below)

3) Given your company's policies and division of duties/tasks, are you required at any time to go head out to look for the runway on this type of approach? (Yes / No)

4) Given your brief exposure to the HUD with synthetic vision and the HDD with synthetic vision, did you form any kind of opinion regarding the potential presence or absence of performance benefits to be gained from either?

5) In your brief exposure to the displays in the post-flights demonstration, did you have any preference for one over the other (yes / no)? If "yes", which one did you have a preference for? (circle one)

HUD with SV / HDD with SV

6) Current consideration of (and the MASPS for) Synthetic Vision Guidance Systems does not require multiple displays (i.e., one on each side of the cockpit). Do you believe that this would be, irrespective of the financial implications:

a) an acceptable installation. or

b) an unacceptable installation and should require duplicate display on FO's side of aircraft?

7) Which of the following do you think would hold true for your company?

a) Task assignment would remain the same regardless of the installation from (6) above.

b) Task assignment might be divided differently with duplicate displays on both sides.

8) Training: What training forms would you want to see for SVG systems? Please rank order the following from 1 (most desired) to 6 (least desired)

Handbook (paper or electronic)	
Computer-based instruction	
Internet (on web site)	
Video (tape or DVD)	
Classroom	
Hands-on in flight simulator	

9) Please indicate, briefly, if you have had any previous experience with Synthetic Vision Systems (terrain depiction) that might influence your opinions on synthetic vision systems:

10) Are there any operations that you believe you could perform with the SVGS that would not have been possible or easily accomplished without it?

Thank you for responding to these questions. The results will be made available to participants when all forms are completed and the results tabulated.

Appendix C. ANOVA Summary Tables

4-factor ANOVA; Glideslope Root-Mean-Squared Error (degrees)

Measure: Glideslope RMSE

Source		Type III Sum of Squares	df	Mean Square	F	Sig.
Display	Sphericity Assumed	.025	2	.013	5.114	.014
	Greenhouse-Geisser	.025	1.383	.018	5.114	.028
	Huynh-Feldt	.025	1.506	.017	5.114	.024
	Lower-bound	.025	1.000	.025	5.114	.043
Error(Display)	Sphericity Assumed	.060	24	.002		
	Greenhouse-Geisser	.060	16.601	.004		
	Huynh-Feldt	.060	18.068	.003		
	Lower-bound	.060	12.000	.005		
RWL	Sphericity Assumed	.000	2	.000	.316	.732
	Greenhouse-Geisser	.000	1.381	.000	.316	.654
	Huynh-Feldt	.000	1.503	.000	.316	.672
	Lower-bound	.000	1.000	.000	.316	.584
Error(RWL)	Sphericity Assumed	.018	24	.001		
	Greenhouse-Geisser	.018	16.577	.001		
	Huynh-Feldt	.018	18.035	.001		
	Lower-bound	.018	12.000	.001		
Illum	Sphericity Assumed	.002	1	.002	2.320	.154
	Greenhouse-Geisser	.002	1.000	.002	2.320	.154
	Huynh-Feldt	.002	1.000	.002	2.320	.154
	Lower-bound	.002	1.000	.002	2.320	.154

Error(Illum)	Sphericity Assumed	.012	12	.001		
	Greenhouse-Geisser	.012	12.000	.001		
	Huynh-Feldt	.012	12.000	.001		
	Lower-bound	.012	12.000	.001		
DH_RVR	Sphericity Assumed	.002	1	.002	1.628	.226
	Greenhouse-Geisser	.002	1.000	.002	1.628	.226
	Huynh-Feldt	.002	1.000	.002	1.628	.226
	Lower-bound	.002	1.000	.002	1.628	.226
Error(DH_RVR)	Sphericity Assumed	.012	12	.001		
	Greenhouse-Geisser	.012	12.000	.001		
	Huynh-Feldt	.012	12.000	.001		
	Lower-bound	.012	12.000	.001		
Display * RWL	Sphericity Assumed	.001	4	.000	.358	.837
	Greenhouse-Geisser	.001	1.705	.001	.358	.670
	Huynh-Feldt	.001	1.959	.001	.358	.699
	Lower-bound	.001	1.000	.001	.358	.561
Error(Display*RWL)	Sphericity Assumed	.036	48	.001		
	Greenhouse-Geisser	.036	20.458	.002		
	Huynh-Feldt	.036	23.502	.002		
	Lower-bound	.036	12.000	.003		
Display * Illum	Sphericity Assumed	.000	2	.000	.260	.774
	Greenhouse-Geisser	.000	1.290	.000	.260	.677
	Huynh-Feldt	.000	1.379	.000	.260	.692
	Lower-bound	.000	1.000	.000	.260	.620
Error(Display*Illum)	Sphericity Assumed	.022	24	.001		

	Greenhouse-Geisser	.022	15.482	.001		
	Huynh-Feldt	.022	16.552	.001		
	Lower-bound	.022	12.000	.002		
RWL * Illum	Sphericity Assumed	.002	2	.001	1.369	.274
	Greenhouse-Geisser	.002	1.742	.001	1.369	.274
	Huynh-Feldt	.002	2.000	.001	1.369	.274
	Lower-bound	.002	1.000	.002	1.369	.265
Error(RWL*Illum)	Sphericity Assumed	.014	24	.001		
	Greenhouse-Geisser	.014	20.900	.001		
	Huynh-Feldt	.014	24.000	.001		
	Lower-bound	.014	12.000	.001		
Display * RWL * Illum	Sphericity Assumed	.002	4	.000	.722	.581
	Greenhouse-Geisser	.002	2.252	.001	.722	.510
	Huynh-Feldt	.002	2.798	.001	.722	.537
	Lower-bound	.002	1.000	.002	.722	.412
Error(Display*RWL*Illum)	Sphericity Assumed	.025	48	.001		
	Greenhouse-Geisser	.025	27.024	.001		
	Huynh-Feldt	.025	33.577	.001		
	Lower-bound	.025	12.000	.002		
Display * DH_RVR	Sphericity Assumed	.001	2	.000	.564	.576
	Greenhouse-Geisser	.001	1.163	.001	.564	.490
	Huynh-Feldt	.001	1.210	.001	.564	.497
	Lower-bound	.001	1.000	.001	.564	.467
Error(Display*DH_RVR)	Sphericity Assumed	.021	24	.001		
	Greenhouse-Geisser	.021	13.950	.001		
	Huynh-Feldt	.021	14.520	.001		

	Lower-bound	.021	12.000	.002		
RWL * DH_RVR	Sphericity Assumed	.001	2	.001	.979	.390
	Greenhouse-Geisser	.001	1.488	.001	.979	.371
	Huynh-Feldt	.001	1.650	.001	.979	.378
	Lower-bound	.001	1.000	.001	.979	.342
Error(RWL*DH_RVR)	Sphericity Assumed	.017	24	.001		
	Greenhouse-Geisser	.017	17.857	.001		
	Huynh-Feldt	.017	19.800	.001		
	Lower-bound	.017	12.000	.001		
Display * RWL * DH_RVR	Sphericity Assumed	.005	4	.001	1.891	.127
	Greenhouse-Geisser	.005	2.531	.002	1.891	.160
	Huynh-Feldt	.005	3.263	.002	1.891	.143
	Lower-bound	.005	1.000	.005	1.891	.194
Error(Display*RWL*DH_RVR)	Sphericity Assumed	.035	48	.001		
	Greenhouse-Geisser	.035	30.371	.001		
	Huynh-Feldt	.035	39.162	.001		
	Lower-bound	.035	12.000	.003		
Illum * DH_RVR	Sphericity Assumed	.000	1	.000	1.034	.329
	Greenhouse-Geisser	.000	1.000	.000	1.034	.329
	Huynh-Feldt	.000	1.000	.000	1.034	.329
	Lower-bound	.000	1.000	.000	1.034	.329
Error(Illum*DH_RVR)	Sphericity Assumed	.005	12	.000		
	Greenhouse-Geisser	.005	12.000	.000		
	Huynh-Feldt	.005	12.000	.000		
	Lower-bound	.005	12.000	.000		
Display * Illum * DH_RVR	Sphericity Assumed	.001	2	.001	1.685	.207

	Greenhouse-Geisser	.001	1.374	.001	1.685	.216
	Huynh-Feldt	.001	1.493	.001	1.685	.215
	Lower-bound	.001	1.000	.001	1.685	.219
Error(Display*Illum*DH_RVR)	Sphericity Assumed	.008	24	.000		
	Greenhouse-Geisser	.008	16.488	.001		
	Huynh-Feldt	.008	17.913	.000		
	Lower-bound	.008	12.000	.001		
RWL * Illum * DH_RVR	Sphericity Assumed	.003	2	.001	2.831	.079
	Greenhouse-Geisser	.003	1.378	.002	2.831	.102
	Huynh-Feldt	.003	1.499	.002	2.831	.097
	Lower-bound	.003	1.000	.003	2.831	.118
Error(RWL*Illum*DH_RVR)	Sphericity Assumed	.011	24	.000		
	Greenhouse-Geisser	.011	16.539	.001		
	Huynh-Feldt	.011	17.982	.001		
	Lower-bound	.011	12.000	.001		
Display * RWL * Illum * DH_RVR	Sphericity Assumed	.001	4	.000	.453	.769
	Greenhouse-Geisser	.001	2.182	.001	.453	.657
	Huynh-Feldt	.001	2.686	.000	.453	.696
	Lower-bound	.001	1.000	.001	.453	.513
Error(Display*RWL*Illum*DH_RVR)	Sphericity Assumed	.029	48	.001		
	Greenhouse-Geisser	.029	26.190	.001		
	Huynh-Feldt	.029	32.235	.001		
	Lower-bound	.029	12.000	.002		

4-factor ANOVA: Localizer Root-Mean-Squared Error (degrees)

Measure: Localizer RMSE

Source		Type III Sum of Squares	df	Mean Square	F	Sig.
Display	Sphericity Assumed	.019	2	.009	12.720	.000
	Greenhouse-Geisser	.019	1.167	.016	12.720	.002
	Huynh-Feldt	.019	1.216	.015	12.720	.002
	Lower-bound	.019	1.000	.019	12.720	.004
Error(Display)	Sphericity Assumed	.018	24	.001		
	Greenhouse-Geisser	.018	14.003	.001		
	Huynh-Feldt	.018	14.588	.001		
	Lower-bound	.018	12.000	.001		
RWL	Sphericity Assumed	.000	2	5.678E-5	.642	.535
	Greenhouse-Geisser	.000	1.628	6.973E-5	.642	.506
	Huynh-Feldt	.000	1.848	6.144E-5	.642	.524
	Lower-bound	.000	1.000	.000	.642	.439
Error(RWL)	Sphericity Assumed	.002	24	8.842E-5		
	Greenhouse-Geisser	.002	19.542	.000		
	Huynh-Feldt	.002	22.181	9.568E-5		
	Lower-bound	.002	12.000	.000		
Illum	Sphericity Assumed	2.180E-5	1	2.180E-5	.086	.774
	Greenhouse-Geisser	2.180E-5	1.000	2.180E-5	.086	.774
	Huynh-Feldt	2.180E-5	1.000	2.180E-5	.086	.774
	Lower-bound	2.180E-5	1.000	2.180E-5	.086	.774
Error(Illum)	Sphericity Assumed	.003	12	.000		
	Greenhouse-Geisser	.003	12.000	.000		

	Huynh-Feldt	.003	12.000	.000		
	Lower-bound	.003	12.000	.000		
DH_RVR	Sphericity Assumed	3.227E-5	1	3.227E-5	.521	.484
	Greenhouse-Geisser	3.227E-5	1.000	3.227E-5	.521	.484
	Huynh-Feldt	3.227E-5	1.000	3.227E-5	.521	.484
	Lower-bound	3.227E-5	1.000	3.227E-5	.521	.484
Error(DH_RVR)	Sphericity Assumed	.001	12	6.195E-5		
	Greenhouse-Geisser	.001	12.000	6.195E-5		
	Huynh-Feldt	.001	12.000	6.195E-5		
	Lower-bound	.001	12.000	6.195E-5		
Display * RWL	Sphericity Assumed	.001	4	.000	3.273	.019
	Greenhouse-Geisser	.001	2.357	.000	3.273	.045
	Huynh-Feldt	.001	2.971	.000	3.273	.033
	Lower-bound	.001	1.000	.001	3.273	.096
Error(Display*RWL)	Sphericity Assumed	.002	48	4.773E-5		
	Greenhouse-Geisser	.002	28.289	8.099E-5		
	Huynh-Feldt	.002	35.649	6.427E-5		
	Lower-bound	.002	12.000	.000		
Display * Illum	Sphericity Assumed	.000	2	7.155E-5	.713	.500
	Greenhouse-Geisser	.000	1.981	7.223E-5	.713	.499
	Huynh-Feldt	.000	2.000	7.155E-5	.713	.500
	Lower-bound	.000	1.000	.000	.713	.415
Error(Display*Illum)	Sphericity Assumed	.002	24	.000		
	Greenhouse-Geisser	.002	23.775	.000		
	Huynh-Feldt	.002	24.000	.000		
	Lower-bound	.002	12.000	.000		

RWL * Illum	Sphericity Assumed	2.576E-5	2	1.288E-5	.255	.777
	Greenhouse-Geisser	2.576E-5	1.746	1.475E-5	.255	.748
	Huynh-Feldt	2.576E-5	2.000	1.288E-5	.255	.777
	Lower-bound	2.576E-5	1.000	2.576E-5	.255	.623
Error(RWL*Illum)	Sphericity Assumed	.001	24	5.054E-5		
	Greenhouse-Geisser	.001	20.956	5.788E-5		
	Huynh-Feldt	.001	24.000	5.054E-5		
	Lower-bound	.001	12.000	.000		
Display * RWL * Illum	Sphericity Assumed	7.155E-5	4	1.789E-5	.293	.881
	Greenhouse-Geisser	7.155E-5	2.840	2.519E-5	.293	.820
	Huynh-Feldt	7.155E-5	3.813	1.876E-5	.293	.873
	Lower-bound	7.155E-5	1.000	7.155E-5	.293	.598
Error(Display*RWL*Illum)	Sphericity Assumed	.003	48	6.101E-5		
	Greenhouse-Geisser	.003	34.086	8.591E-5		
	Huynh-Feldt	.003	45.758	6.400E-5		
	Lower-bound	.003	12.000	.000		
Display * DH_RVR	Sphericity Assumed	.000	2	5.822E-5	.406	.671
	Greenhouse-Geisser	.000	1.811	6.431E-5	.406	.651
	Huynh-Feldt	.000	2.000	5.822E-5	.406	.671
	Lower-bound	.000	1.000	.000	.406	.536
Error(Display*DH_RVR)	Sphericity Assumed	.003	24	.000		
	Greenhouse-Geisser	.003	21.729	.000		
	Huynh-Feldt	.003	24.000	.000		
	Lower-bound	.003	12.000	.000		
RWL * DH_RVR	Sphericity Assumed	6.122E-5	2	3.061E-5	.224	.801

	Greenhouse-Geisser	6.122E-5	1.548	3.955E-5	.224	.745
	Huynh-Feldt	6.122E-5	1.734	3.531E-5	.224	.771
	Lower-bound	6.122E-5	1.000	6.122E-5	.224	.645
Error(RWL*DH_RVR)	Sphericity Assumed	.003	24	.000		
	Greenhouse-Geisser	.003	18.573	.000		
	Huynh-Feldt	.003	20.804	.000		
	Lower-bound	.003	12.000	.000		
Display * RWL * DH_RVR	Sphericity Assumed	.001	4	.000	.795	.534
	Greenhouse-Geisser	.001	1.598	.001	.795	.440
	Huynh-Feldt	.001	1.804	.001	.795	.452
	Lower-bound	.001	1.000	.001	.795	.390
Error(Display*RWL*DH_RVR)	Sphericity Assumed	.020	48	.000		
	Greenhouse-Geisser	.020	19.171	.001		
	Huynh-Feldt	.020	21.651	.001		
	Lower-bound	.020	12.000	.002		
Illum * DH_RVR	Sphericity Assumed	3.202E-6	1	3.202E-6	.058	.813
	Greenhouse-Geisser	3.202E-6	1.000	3.202E-6	.058	.813
	Huynh-Feldt	3.202E-6	1.000	3.202E-6	.058	.813
	Lower-bound	3.202E-6	1.000	3.202E-6	.058	.813
Error(Illum*DH_RVR)	Sphericity Assumed	.001	12	5.506E-5		
	Greenhouse-Geisser	.001	12.000	5.506E-5		
	Huynh-Feldt	.001	12.000	5.506E-5		
	Lower-bound	.001	12.000	5.506E-5		
Display * Illum * DH_RVR	Sphericity Assumed	6.108E-5	2	3.054E-5	.451	.642
	Greenhouse-Geisser	6.108E-5	1.966	3.107E-5	.451	.639
	Huynh-Feldt	6.108E-5	2.000	3.054E-5	.451	.642

	Lower-bound	6.108E-5	1.000	6.108E-5	.451	.515
Error(Display*Illum*DH_RVR)	Sphericity Assumed	.002	24	6.776E-5		
	Greenhouse-Geisser	.002	23.587	6.895E-5		
	Huynh-Feldt	.002	24.000	6.776E-5		
	Lower-bound	.002	12.000	.000		
RWL * Illum * DH_RVR	Sphericity Assumed	.000	2	.000	2.264	.126
	Greenhouse-Geisser	.000	1.388	.000	2.264	.146
	Huynh-Feldt	.000	1.512	.000	2.264	.142
	Lower-bound	.000	1.000	.000	2.264	.158
Error(RWL*Illum*DH_RVR)	Sphericity Assumed	.002	24	9.891E-5		
	Greenhouse-Geisser	.002	16.658	.000		
	Huynh-Feldt	.002	18.145	.000		
	Lower-bound	.002	12.000	.000		
Display * RWL * Illum * DH_RVR	Sphericity Assumed	.001	4	.000	1.706	.164
	Greenhouse-Geisser	.001	2.102	.000	1.706	.201
	Huynh-Feldt	.001	2.558	.000	1.706	.192
	Lower-bound	.001	1.000	.001	1.706	.216
Error(Display*RWL*Illum*DH_RVR)	Sphericity Assumed	.004	48	8.775E-5		
	Greenhouse-Geisser	.004	25.222	.000		
	Huynh-Feldt	.004	30.701	.000		
	Lower-bound	.004	12.000	.000		

Sampling variable ANOVA: Wind Direction Effect on Altitude at Runway Visual Acquisition

Measure: Altitude at Runway Visual Acquisition

Source		Type III Sum of Squares	df	Mean Square	F	Sig.
Wind	Sphericity Assumed	960.520	2	480.260	6.500	.006
	Greenhouse-Geisser	960.520	1.659	578.903	6.500	.009
	Huynh-Feldt	960.520	1.892	507.547	6.500	.007
	Lower-bound	960.520	1.000	960.520	6.500	.025
Error(Wind)	Sphericity Assumed	1773.233	24	73.885		
	Greenhouse-Geisser	1773.233	19.910	89.060		
	Huynh-Feldt	1773.233	22.710	78.083		
	Lower-bound	1773.233	12.000	147.769		

4-factor ANOVA: Mean Sea Level Altitude at Runway Visual Acquisition (MSL, ft)

Measure: Altitude at Runway Visual Acquisition

Source		Type III Sum of Squares	df	Mean Square	F	Sig.
Display	Sphericity Assumed	40953.903	2	20476.951	17.300	.000
	Greenhouse-Geisser	40953.903	1.945	21059.887	17.300	.000
	Huynh-Feldt	40953.903	2.000	20476.951	17.300	.000
	Lower-bound	40953.903	1.000	40953.903	17.300	.001
Error(Display)	Sphericity Assumed	28406.631	24	1183.610		
	Greenhouse-Geisser	28406.631	23.336	1217.304		
	Huynh-Feldt	28406.631	24.000	1183.610		
	Lower-bound	28406.631	12.000	2367.219		
RWL	Sphericity Assumed	1198.297	2	599.148	.940	.405
	Greenhouse-Geisser	1198.297	1.599	749.229	.940	.388
	Huynh-Feldt	1198.297	1.807	663.215	.940	.397
	Lower-bound	1198.297	1.000	1198.297	.940	.351
Error(RWL)	Sphericity Assumed	15301.536	24	637.564		
	Greenhouse-Geisser	15301.536	19.192	797.267		
	Huynh-Feldt	15301.536	21.682	705.738		

	Lower-bound	15301.536	12.000	1275.128		
Illum	Sphericity Assumed	15423.852	1	15423.852	4.841	.048
	Greenhouse-Geisser	15423.852	1.000	15423.852	4.841	.048
	Huynh-Feldt	15423.852	1.000	15423.852	4.841	.048
	Lower-bound	15423.852	1.000	15423.852	4.841	.048
Error(Illum)	Sphericity Assumed	38231.846	12	3185.987		
	Greenhouse-Geisser	38231.846	12.000	3185.987		
	Huynh-Feldt	38231.846	12.000	3185.987		
	Lower-bound	38231.846	12.000	3185.987		
DH_RVR	Sphericity Assumed	52689.624	1	52689.624	55.859	.000
	Greenhouse-Geisser	52689.624	1.000	52689.624	55.859	.000
	Huynh-Feldt	52689.624	1.000	52689.624	55.859	.000
	Lower-bound	52689.624	1.000	52689.624	55.859	.000
Error(DH_RVR)	Sphericity Assumed	11319.052	12	943.254		
	Greenhouse-Geisser	11319.052	12.000	943.254		
	Huynh-Feldt	11319.052	12.000	943.254		
	Lower-bound	11319.052	12.000	943.254		
Display * RWL	Sphericity Assumed	1220.549	4	305.137	.342	.848
	Greenhouse-Geisser	1220.549	1.678	727.343	.342	.677

	Huynh-Feldt	1220.549	1.920	635.795	.342	.705
	Lower-bound	1220.549	1.000	1220.549	.342	.570
Error(Display*RWL)	Sphericity Assumed	42837.426	48	892.446		
	Greenhouse-Geisser	42837.426	20.137	2127.289		
	Huynh-Feldt	42837.426	23.037	1859.533		
	Lower-bound	42837.426	12.000	3569.786		
Display * Illum	Sphericity Assumed	343.249	2	171.624	.175	.841
	Greenhouse-Geisser	343.249	1.445	237.508	.175	.771
	Huynh-Feldt	343.249	1.591	215.808	.175	.792
	Lower-bound	343.249	1.000	343.249	.175	.683
Error(Display*Illum)	Sphericity Assumed	23578.206	24	982.425		
	Greenhouse-Geisser	23578.206	17.342	1359.562		
	Huynh-Feldt	23578.206	19.086	1235.344		
	Lower-bound	23578.206	12.000	1964.851		
RWL * Illum	Sphericity Assumed	1234.086	2	617.043	.657	.528
	Greenhouse-Geisser	1234.086	1.339	921.669	.657	.473
	Huynh-Feldt	1234.086	1.445	853.961	.657	.483
	Lower-bound	1234.086	1.000	1234.086	.657	.434
Error(RWL*Illum)	Sphericity Assumed	22556.988	24	939.874		

	Greenhouse-Geisser	22556.988	16.068	1403.878		
	Huynh-Feldt	22556.988	17.342	1300.746		
	Lower-bound	22556.988	12.000	1879.749		
Display * RWL * Illum	Sphericity Assumed	5999.185	4	1499.796	1.655	.176
	Greenhouse-Geisser	5999.185	2.096	2861.608	1.655	.210
	Huynh-Feldt	5999.185	2.550	2352.658	1.655	.202
	Lower-bound	5999.185	1.000	5999.185	1.655	.223
Error(Display*RWL*Illum)	Sphericity Assumed	43495.499	48	906.156		
	Greenhouse-Geisser	43495.499	25.157	1728.944		
	Huynh-Feldt	43495.499	30.600	1421.443		
	Lower-bound	43495.499	12.000	3624.625		
Display * DH_RVR	Sphericity Assumed	101.568	2	50.784	.041	.960
	Greenhouse-Geisser	101.568	1.387	73.217	.041	.908
	Huynh-Feldt	101.568	1.511	67.228	.041	.923
	Lower-bound	101.568	1.000	101.568	.041	.842
Error(Display*DH_RVR)	Sphericity Assumed	29466.916	24	1227.788		
	Greenhouse-Geisser	29466.916	16.647	1770.139		
	Huynh-Feldt	29466.916	18.130	1625.338		
	Lower-bound	29466.916	12.000	2455.576		

RWL * DH_RVR	Sphericity Assumed	2945.052	2	1472.526	1.801	.187
	Greenhouse-Geisser	2945.052	1.582	1861.342	1.801	.196
	Huynh-Feldt	2945.052	1.782	1652.278	1.801	.191
	Lower-bound	2945.052	1.000	2945.052	1.801	.204
Error(RWL*DH_RVR)	Sphericity Assumed	19621.131	24	817.547		
	Greenhouse-Geisser	19621.131	18.987	1033.418		
	Huynh-Feldt	19621.131	21.389	917.345		
	Lower-bound	19621.131	12.000	1635.094		
Display * RWL * DH_RVR	Sphericity Assumed	2644.650	4	661.162	.598	.666
	Greenhouse-Geisser	2644.650	2.197	1203.626	.598	.572
	Huynh-Feldt	2644.650	2.710	975.938	.598	.605
	Lower-bound	2644.650	1.000	2644.650	.598	.454
Error(Display*RWL*DH_RVR)	Sphericity Assumed	53094.179	48	1106.129		
	Greenhouse-Geisser	53094.179	26.367	2013.674		
	Huynh-Feldt	53094.179	32.518	1632.750		
	Lower-bound	53094.179	12.000	4424.515		
Illum * DH_RVR	Sphericity Assumed	12.306	1	12.306	.018	.896
	Greenhouse-Geisser	12.306	1.000	12.306	.018	.896
	Huynh-Feldt	12.306	1.000	12.306	.018	.896

	Lower-bound	12.306	1.000	12.306	.018	.896
Error(Illum*DH_RVR)	Sphericity Assumed	8221.786	12	685.149		
	Greenhouse-Geisser	8221.786	12.000	685.149		
	Huynh-Feldt	8221.786	12.000	685.149		
	Lower-bound	8221.786	12.000	685.149		
Display * Illum * DH_RVR	Sphericity Assumed	1339.820	2	669.910	.908	.417
	Greenhouse-Geisser	1339.820	1.628	822.792	.908	.401
	Huynh-Feldt	1339.820	1.848	724.927	.908	.411
	Lower-bound	1339.820	1.000	1339.820	.908	.359
Error(Display*Illum*DH_RVR)	Sphericity Assumed	17710.121	24	737.922		
	Greenhouse-Geisser	17710.121	19.541	906.325		
	Huynh-Feldt	17710.121	22.179	798.524		
	Lower-bound	17710.121	12.000	1475.843		
RWL * Illum * DH_RVR	Sphericity Assumed	855.433	2	427.717	.526	.598
	Greenhouse-Geisser	855.433	1.173	729.109	.526	.508
	Huynh-Feldt	855.433	1.224	698.861	.526	.515
	Lower-bound	855.433	1.000	855.433	.526	.482
Error(RWL*Illum*DH_RVR)	Sphericity Assumed	19517.818	24	813.242		
	Greenhouse-Geisser	19517.818	14.079	1386.297		

	Huynh-Feldt	19517.818	14.688	1328.785		
	Lower-bound	19517.818	12.000	1626.485		
Display * RWL * Illum * DH_RVR	Sphericity Assumed	5309.970	4	1327.492	1.366	.260
	Greenhouse-Geisser	5309.970	2.411	2202.146	1.366	.273
	Huynh-Feldt	5309.970	3.061	1734.988	1.366	.268
	Lower-bound	5309.970	1.000	5309.970	1.366	.265
Error(Display*RWL*Illum*DH_RVR)	Sphericity Assumed	46655.668	48	971.993		
	Greenhouse-Geisser	46655.668	28.935	1612.416		
	Huynh-Feldt	46655.668	36.726	1270.362		
	Lower-bound	46655.668	12.000	3887.972		

4-factor ANOVA: Distance to Touchdown Zone (Dist_TDZ, ft)

Measure: Distance to Touchdown Zone, Along runway major axis

Source		Type III Sum of Squares	df	Mean Square	F	Sig.
Display	Sphericity Assumed	20354.030	2	10177.015	.023	.977
	Greenhouse-Geisser	20354.030	1.632	12468.323	.023	.958
	Huynh-Feldt	20354.030	1.854	10978.127	.023	.971
	Lower-bound	20354.030	1.000	20354.030	.023	.881
Error(Display)	Sphericity Assumed	10429295.443	24	434553.977		
	Greenhouse-Geisser	10429295.443	19.590	532391.785		

	Huynh-Feldt	10429295.443	22.249	468761.070		
	Lower-bound	10429295.443	12.000	869107.954		
RWL	Sphericity Assumed	203093.172	2	101546.586	1.898	.172
	Greenhouse-Geisser	203093.172	1.322	153660.724	1.898	.188
	Huynh-Feldt	203093.172	1.422	142845.364	1.898	.186
	Lower-bound	203093.172	1.000	203093.172	1.898	.193
Error(RWL)	Sphericity Assumed	1284123.094	24	53505.129		
	Greenhouse-Geisser	1284123.094	15.860	80964.188		
	Huynh-Feldt	1284123.094	17.061	75265.550		
	Lower-bound	1284123.094	12.000	107010.258		
Illum	Sphericity Assumed	1108157.432	1	1108157.432	14.544	.002
	Greenhouse-Geisser	1108157.432	1.000	1108157.432	14.544	.002
	Huynh-Feldt	1108157.432	1.000	1108157.432	14.544	.002
	Lower-bound	1108157.432	1.000	1108157.432	14.544	.002
Error(Illum)	Sphericity Assumed	914344.728	12	76195.394		
	Greenhouse-Geisser	914344.728	12.000	76195.394		
	Huynh-Feldt	914344.728	12.000	76195.394		
	Lower-bound	914344.728	12.000	76195.394		

DH_RVR	Sphericity Assumed	1788.383	1	1788.383	.038	.848
	Greenhouse-Geisser	1788.383	1.000	1788.383	.038	.848
	Huynh-Feldt	1788.383	1.000	1788.383	.038	.848
	Lower-bound	1788.383	1.000	1788.383	.038	.848
Error(DH_RVR)	Sphericity Assumed	559452.586	12	46621.049		
	Greenhouse-Geisser	559452.586	12.000	46621.049		
	Huynh-Feldt	559452.586	12.000	46621.049		
	Lower-bound	559452.586	12.000	46621.049		
Display * RWL	Sphericity Assumed	227132.394	4	56783.098	1.045	.394
	Greenhouse-Geisser	227132.394	2.336	97229.414	1.045	.374
	Huynh-Feldt	227132.394	2.936	77374.176	1.045	.384
	Lower-bound	227132.394	1.000	227132.394	1.045	.327
Error(Display*RWL)	Sphericity Assumed	2608551.798	48	54344.829		
	Greenhouse-Geisser	2608551.798	28.033	93054.378		
	Huynh-Feldt	2608551.798	35.226	74051.724		
	Lower-bound	2608551.798	12.000	217379.316		
Display * Illum	Sphericity Assumed	20063.808	2	10031.904	.111	.895
	Greenhouse-Geisser	20063.808	1.992	10070.508	.111	.894

	Huynh-Feldt	20063.808	2.000	10031.904	.111	.895
	Lower-bound	20063.808	1.000	20063.808	.111	.744
Error(Display*Illum)	Sphericity Assumed	2163340.044	24	90139.169		
	Greenhouse-Geisser	2163340.044	23.908	90486.037		
	Huynh-Feldt	2163340.044	24.000	90139.169		
	Lower-bound	2163340.044	12.000	180278.337		
RWL * Illum	Sphericity Assumed	146936.483	2	73468.241	.707	.503
	Greenhouse-Geisser	146936.483	1.850	79441.715	.707	.493
	Huynh-Feldt	146936.483	2.000	73468.241	.707	.503
	Lower-bound	146936.483	1.000	146936.483	.707	.417
Error(RWL*Illum)	Sphericity Assumed	2494203.289	24	103925.137		
	Greenhouse-Geisser	2494203.289	22.195	112374.965		
	Huynh-Feldt	2494203.289	24.000	103925.137		
	Lower-bound	2494203.289	12.000	207850.274		
Display * RWL * Illum	Sphericity Assumed	345119.829	4	86279.957	.925	.457
	Greenhouse-Geisser	345119.829	3.224	107063.531	.925	.443
	Huynh-Feldt	345119.829	4.000	86279.957	.925	.457
	Lower-bound	345119.829	1.000	345119.829	.925	.355

Error(Display*RWL*Illum)	Sphericity Assumed	4477057.005	48	93272.021		
	Greenhouse-Geisser	4477057.005	38.682	115739.881		
	Huynh-Feldt	4477057.005	48.000	93272.021		
	Lower-bound	4477057.005	12.000	373088.084		
Display * DH_RVR	Sphericity Assumed	95018.214	2	47509.107	.601	.556
	Greenhouse-Geisser	95018.214	1.625	58454.883	.601	.525
	Huynh-Feldt	95018.214	1.844	51525.968	.601	.544
	Lower-bound	95018.214	1.000	95018.214	.601	.453
Error(Display*DH_RVR)	Sphericity Assumed	1895896.472	24	78995.686		
	Greenhouse-Geisser	1895896.472	19.506	97195.756		
	Huynh-Feldt	1895896.472	22.129	85674.714		
	Lower-bound	1895896.472	12.000	157991.373		
RWL * DH_RVR	Sphericity Assumed	537917.606	2	268958.803	1.824	.183
	Greenhouse-Geisser	537917.606	1.441	373212.388	1.824	.195
	Huynh-Feldt	537917.606	1.585	339347.383	1.824	.192
	Lower-bound	537917.606	1.000	537917.606	1.824	.202
Error(RWL*DH_RVR)	Sphericity Assumed	3539594.118	24	147483.088		
	Greenhouse-Geisser	3539594.118	17.296	204650.359		

	Huynh-Feldt	3539594.118	19.022	186080.543		
	Lower-bound	3539594.118	12.000	294966.177		
Display * RWL * DH_RVR	Sphericity Assumed	37412.064	4	9353.016	.057	.994
	Greenhouse-Geisser	37412.064	1.827	20481.800	.057	.932
	Huynh-Feldt	37412.064	2.138	17502.588	.057	.952
	Lower-bound	37412.064	1.000	37412.064	.057	.815
Error(Display*RWL*DH_RVR)	Sphericity Assumed	7835239.461	48	163234.155		
	Greenhouse-Geisser	7835239.461	21.919	357460.022		
	Huynh-Feldt	7835239.461	25.650	305465.127		
	Lower-bound	7835239.461	12.000	652936.622		
Illum * DH_RVR	Sphericity Assumed	14944.725	1	14944.725	.151	.704
	Greenhouse-Geisser	14944.725	1.000	14944.725	.151	.704
	Huynh-Feldt	14944.725	1.000	14944.725	.151	.704
	Lower-bound	14944.725	1.000	14944.725	.151	.704
Error(Illum*DH_RVR)	Sphericity Assumed	1187454.773	12	98954.564		
	Greenhouse-Geisser	1187454.773	12.000	98954.564		
	Huynh-Feldt	1187454.773	12.000	98954.564		
	Lower-bound	1187454.773	12.000	98954.564		

Display * Illum * DH_RVR	Sphericity Assumed	153145.346	2	76572.673	1.069	.359
	Greenhouse-Geisser	153145.346	1.475	103832.091	1.069	.344
	Huynh-Feldt	153145.346	1.632	93854.277	1.069	.349
	Lower-bound	153145.346	1.000	153145.346	1.069	.321
Error(Display*Illum*DH_RVR)	Sphericity Assumed	1718437.776	24	71601.574		
	Greenhouse-Geisser	1718437.776	17.699	97091.311		
	Huynh-Feldt	1718437.776	19.581	87761.256		
	Lower-bound	1718437.776	12.000	143203.148		
RWL * Illum * DH_RVR	Sphericity Assumed	99252.785	2	49626.393	.576	.570
	Greenhouse-Geisser	99252.785	1.958	50699.984	.576	.566
	Huynh-Feldt	99252.785	2.000	49626.393	.576	.570
	Lower-bound	99252.785	1.000	99252.785	.576	.462
Error(RWL*Illum*DH_RVR)	Sphericity Assumed	2067365.161	24	86140.215		
	Greenhouse-Geisser	2067365.161	23.492	88003.728		
	Huynh-Feldt	2067365.161	24.000	86140.215		
	Lower-bound	2067365.161	12.000	172280.430		
Display * RWL * Illum * DH_RVR	Sphericity Assumed	238280.319	4	59570.080	.998	.418
	Greenhouse-Geisser	238280.319	2.690	88596.277	.998	.399

	Huynh-Feldt	238280.319	3.540	67301.742	.998	.413
	Lower-bound	238280.319	1.000	238280.319	.998	.337
Error(Display*RWL*Illum*DH_RVR)	Sphericity Assumed	2864644.565	48	59680.095		
	Greenhouse-Geisser	2864644.565	32.274	88759.899		
	Huynh-Feldt	2864644.565	42.486	67426.036		
	Lower-bound	2864644.565	12.000	238720.380		

4-factor ANOVA: Distance from Centerline (Dist_CL, ft)

Measure: Distance from Centerline

Source		Type III Sum of Squares	df	Mean Square	F	Sig.
Display	Sphericity Assumed	8059.969	2	4029.984	24.772	.000
	Greenhouse-Geisser	8059.969	1.686	4781.836	24.772	.000
	Huynh-Feldt	8059.969	1.930	4175.082	24.772	.000
	Lower-bound	8059.969	1.000	8059.969	24.772	.000
Error(Display)	Sphericity Assumed	3904.347	24	162.681		
	Greenhouse-Geisser	3904.347	20.226	193.032		
	Huynh-Feldt	3904.347	23.166	168.538		
	Lower-bound	3904.347	12.000	325.362		
RWL	Sphericity Assumed	48.562	2	24.281	.314	.733
	Greenhouse-Geisser	48.562	1.534	31.661	.314	.677
	Huynh-Feldt	48.562	1.714	28.332	.314	.701
	Lower-bound	48.562	1.000	48.562	.314	.585
Error(RWL)	Sphericity Assumed	1854.608	24	77.275		
	Greenhouse-Geisser	1854.608	18.405	100.764		
	Huynh-Feldt	1854.608	20.568	90.169		
	Lower-bound	1854.608	12.000	154.551		

Illum	Sphericity Assumed	97.366	1	97.366	1.310	.275
	Greenhouse-Geisser	97.366	1.000	97.366	1.310	.275
	Huynh-Feldt	97.366	1.000	97.366	1.310	.275
	Lower-bound	97.366	1.000	97.366	1.310	.275
Error(Illum)	Sphericity Assumed	891.911	12	74.326		
	Greenhouse-Geisser	891.911	12.000	74.326		
	Huynh-Feldt	891.911	12.000	74.326		
	Lower-bound	891.911	12.000	74.326		
DH_RVR	Sphericity Assumed	173.502	1	173.502	2.249	.160
	Greenhouse-Geisser	173.502	1.000	173.502	2.249	.160
	Huynh-Feldt	173.502	1.000	173.502	2.249	.160
	Lower-bound	173.502	1.000	173.502	2.249	.160
Error(DH_RVR)	Sphericity Assumed	925.723	12	77.144		
	Greenhouse-Geisser	925.723	12.000	77.144		
	Huynh-Feldt	925.723	12.000	77.144		
	Lower-bound	925.723	12.000	77.144		
Display * RWL	Sphericity Assumed	324.533	4	81.133	.917	.462
	Greenhouse-Geisser	324.533	2.572	126.174	.917	.432
	Huynh-Feldt	324.533	3.335	97.326	.917	.450

	Lower-bound	324.533	1.000	324.533	.917	.357
Error(Display*RWL)	Sphericity Assumed	4245.637	48	88.451		
	Greenhouse-Geisser	4245.637	30.865	137.554		
	Huynh-Feldt	4245.637	40.014	106.104		
	Lower-bound	4245.637	12.000	353.803		
Display * Illum	Sphericity Assumed	121.830	2	60.915	.957	.398
	Greenhouse-Geisser	121.830	1.106	110.179	.957	.355
	Huynh-Feldt	121.830	1.136	107.255	.957	.357
	Lower-bound	121.830	1.000	121.830	.957	.347
Error(Display*Illum)	Sphericity Assumed	1528.019	24	63.667		
	Greenhouse-Geisser	1528.019	13.269	115.158		
	Huynh-Feldt	1528.019	13.631	112.102		
	Lower-bound	1528.019	12.000	127.335		
RWL * Illum	Sphericity Assumed	4.526	2	2.263	.037	.964
	Greenhouse-Geisser	4.526	1.881	2.406	.037	.957
	Huynh-Feldt	4.526	2.000	2.263	.037	.964
	Lower-bound	4.526	1.000	4.526	.037	.851
Error(RWL*Illum)	Sphericity Assumed	1472.442	24	61.352		
	Greenhouse-Geisser	1472.442	22.573	65.230		

	Huynh-Feldt	1472.442	24.000	61.352		
	Lower-bound	1472.442	12.000	122.703		
Display * RWL * Illum	Sphericity Assumed	100.391	4	25.098	.433	.784
	Greenhouse-Geisser	100.391	2.768	36.271	.433	.715
	Huynh-Feldt	100.391	3.681	27.274	.433	.769
	Lower-bound	100.391	1.000	100.391	.433	.523
Error(Display*RWL*Illum)	Sphericity Assumed	2780.735	48	57.932		
	Greenhouse-Geisser	2780.735	33.214	83.722		
	Huynh-Feldt	2780.735	44.169	62.956		
	Lower-bound	2780.735	12.000	231.728		
Display * DH_RVR	Sphericity Assumed	67.375	2	33.688	.088	.916
	Greenhouse-Geisser	67.375	1.230	54.790	.088	.821
	Huynh-Feldt	67.375	1.299	51.883	.088	.833
	Lower-bound	67.375	1.000	67.375	.088	.771
Error(Display*DH_RVR)	Sphericity Assumed	9161.862	24	381.744		
	Greenhouse-Geisser	9161.862	14.757	620.868		
	Huynh-Feldt	9161.862	15.583	587.934		
	Lower-bound	9161.862	12.000	763.488		
RWL * DH_RVR	Sphericity Assumed	30.773	2	15.387	.038	.963

	Greenhouse-Geisser	30.773	1.167	26.376	.038	.882
	Huynh-Feldt	30.773	1.215	25.319	.038	.890
	Lower-bound	30.773	1.000	30.773	.038	.849
Error(RWL*DH_RVR)	Sphericity Assumed	9753.294	24	406.387		
	Greenhouse-Geisser	9753.294	14.001	696.633		
	Huynh-Feldt	9753.294	14.585	668.701		
	Lower-bound	9753.294	12.000	812.775		
Display * RWL * DH_RVR	Sphericity Assumed	330.312	4	82.578	.069	.991
	Greenhouse-Geisser	330.312	1.125	293.587	.069	.825
	Huynh-Feldt	330.312	1.161	284.497	.069	.833
	Lower-bound	330.312	1.000	330.312	.069	.797
Error(Display*RWL*DH_RVR)	Sphericity Assumed	57576.719	48	1199.515		
	Greenhouse-Geisser	57576.719	13.501	4264.594		
	Huynh-Feldt	57576.719	13.932	4132.556		
	Lower-bound	57576.719	12.000	4798.060		
Illum * DH_RVR	Sphericity Assumed	172.081	1	172.081	3.460	.088
	Greenhouse-Geisser	172.081	1.000	172.081	3.460	.088
	Huynh-Feldt	172.081	1.000	172.081	3.460	.088
	Lower-bound	172.081	1.000	172.081	3.460	.088

Error(Illum*DH_RVR)	Sphericity Assumed	596.854	12	49.738		
	Greenhouse-Geisser	596.854	12.000	49.738		
	Huynh-Feldt	596.854	12.000	49.738		
	Lower-bound	596.854	12.000	49.738		
Display * Illum * DH_RVR	Sphericity Assumed	650.076	2	325.038	4.920	.016
	Greenhouse-Geisser	650.076	1.578	412.034	4.920	.025
	Huynh-Feldt	650.076	1.776	366.025	4.920	.020
	Lower-bound	650.076	1.000	650.076	4.920	.047
Error(Display*Illum*DH_RVR)	Sphericity Assumed	1585.482	24	66.062		
	Greenhouse-Geisser	1585.482	18.933	83.743		
	Huynh-Feldt	1585.482	21.313	74.392		
	Lower-bound	1585.482	12.000	132.124		
RWL * Illum * DH_RVR	Sphericity Assumed	59.096	2	29.548	.409	.669
	Greenhouse-Geisser	59.096	1.884	31.375	.409	.657
	Huynh-Feldt	59.096	2.000	29.548	.409	.669
	Lower-bound	59.096	1.000	59.096	.409	.534
Error(RWL*Illum*DH_RVR)	Sphericity Assumed	1732.465	24	72.186		
	Greenhouse-Geisser	1732.465	22.603	76.648		
	Huynh-Feldt	1732.465	24.000	72.186		

	Lower-bound	1732.465	12.000	144.372		
Display * RWL * Illum * DH_RVR	Sphericity Assumed	658.923	4	164.731	2.564	.050
	Greenhouse-Geisser	658.923	2.676	246.262	2.564	.078
	Huynh-Feldt	658.923	3.516	187.408	2.564	.059
	Lower-bound	658.923	1.000	658.923	2.564	.135
Error(Display*RWL*Illum*DH_RVR)	Sphericity Assumed	3083.565	48	64.241		
	Greenhouse-Geisser	3083.565	32.108	96.036		
	Huynh-Feldt	3083.565	42.192	73.084		
	Lower-bound	3083.565	12.000	256.964		

4-factor ANOVA: Vertical Velocity just before runway contact (VV, ft/sec, "–" down)

Measure: Vertical Velocity

Source		Type III Sum of Squares	df	Mean Square	F	Sig.
Display	Sphericity Assumed	47.919	2	23.960	3.000	.069
	Greenhouse-Geisser	47.919	1.824	26.268	3.000	.075
	Huynh-Feldt	47.919	2.000	23.960	3.000	.069
	Lower-bound	47.919	1.000	47.919	3.000	.109
Error(Display)	Sphericity Assumed	191.672	24	7.986		
	Greenhouse-Geisser	191.672	21.891	8.756		
	Huynh-Feldt	191.672	24.000	7.986		
	Lower-bound	191.672	12.000	15.973		
RWL	Sphericity Assumed	5.846	2	2.923	1.000	.383
	Greenhouse-Geisser	5.846	1.719	3.401	1.000	.374
	Huynh-Feldt	5.846	1.979	2.954	1.000	.382
	Lower-bound	5.846	1.000	5.846	1.000	.337
Error(RWL)	Sphericity Assumed	70.176	24	2.924		
	Greenhouse-Geisser	70.176	20.624	3.403		
	Huynh-Feldt	70.176	23.744	2.956		

	Lower-bound	70.176	12.000	5.848		
Illum	Sphericity Assumed	15.025	1	15.025	4.187	.063
	Greenhouse-Geisser	15.025	1.000	15.025	4.187	.063
	Huynh-Feldt	15.025	1.000	15.025	4.187	.063
	Lower-bound	15.025	1.000	15.025	4.187	.063
Error(Illum)	Sphericity Assumed	43.062	12	3.588		
	Greenhouse-Geisser	43.062	12.000	3.588		
	Huynh-Feldt	43.062	12.000	3.588		
	Lower-bound	43.062	12.000	3.588		
DH_RVR	Sphericity Assumed	2.746	1	2.746	1.095	.316
	Greenhouse-Geisser	2.746	1.000	2.746	1.095	.316
	Huynh-Feldt	2.746	1.000	2.746	1.095	.316
	Lower-bound	2.746	1.000	2.746	1.095	.316
Error(DH_RVR)	Sphericity Assumed	30.089	12	2.507		
	Greenhouse-Geisser	30.089	12.000	2.507		
	Huynh-Feldt	30.089	12.000	2.507		
	Lower-bound	30.089	12.000	2.507		
Display * RWL	Sphericity Assumed	17.908	4	4.477	2.211	.082

	Greenhouse-Geisser	17.908	2.729	6.562	2.211	.111
	Huynh-Feldt	17.908	3.611	4.959	2.211	.090
	Lower-bound	17.908	1.000	17.908	2.211	.163
Error(Display*RWL)	Sphericity Assumed	97.200	48	2.025		
	Greenhouse-Geisser	97.200	32.750	2.968		
	Huynh-Feldt	97.200	43.334	2.243		
	Lower-bound	97.200	12.000	8.100		
Display * Illum	Sphericity Assumed	19.418	2	9.709	2.693	.088
	Greenhouse-Geisser	19.418	1.589	12.224	2.693	.103
	Huynh-Feldt	19.418	1.791	10.839	2.693	.095
	Lower-bound	19.418	1.000	19.418	2.693	.127
Error(Display*Illum)	Sphericity Assumed	86.519	24	3.605		
	Greenhouse-Geisser	86.519	19.063	4.539		
	Huynh-Feldt	86.519	21.497	4.025		
	Lower-bound	86.519	12.000	7.210		
RWL * Illum	Sphericity Assumed	.721	2	.360	.142	.868
	Greenhouse-Geisser	.721	1.607	.448	.142	.824
	Huynh-Feldt	.721	1.818	.396	.142	.850

	Lower-bound	.721	1.000	.721	.142	.713
Error(RWL*Illum)	Sphericity Assumed	60.918	24	2.538		
	Greenhouse-Geisser	60.918	19.288	3.158		
	Huynh-Feldt	60.918	21.818	2.792		
	Lower-bound	60.918	12.000	5.076		
Display * RWL * Illum	Sphericity Assumed	15.219	4	3.805	1.889	.128
	Greenhouse-Geisser	15.219	2.741	5.552	1.889	.155
	Huynh-Feldt	15.219	3.632	4.190	1.889	.135
	Lower-bound	15.219	1.000	15.219	1.889	.194
Error(Display*RWL*Illum)	Sphericity Assumed	96.699	48	2.015		
	Greenhouse-Geisser	96.699	32.891	2.940		
	Huynh-Feldt	96.699	43.588	2.218		
	Lower-bound	96.699	12.000	8.058		
Display * DH_RVR	Sphericity Assumed	7.213	2	3.607	1.871	.176
	Greenhouse-Geisser	7.213	1.842	3.917	1.871	.180
	Huynh-Feldt	7.213	2.000	3.607	1.871	.176
	Lower-bound	7.213	1.000	7.213	1.871	.196
Error(Display*DH_RVR)	Sphericity Assumed	46.275	24	1.928		

	Greenhouse-Geisser	46.275	22.098	2.094		
	Huynh-Feldt	46.275	24.000	1.928		
	Lower-bound	46.275	12.000	3.856		
RWL * DH_RVR	Sphericity Assumed	3.907	2	1.954	1.608	.221
	Greenhouse-Geisser	3.907	1.766	2.213	1.608	.224
	Huynh-Feldt	3.907	2.000	1.954	1.608	.221
	Lower-bound	3.907	1.000	3.907	1.608	.229
Error(RWL*DH_RVR)	Sphericity Assumed	29.153	24	1.215		
	Greenhouse-Geisser	29.153	21.191	1.376		
	Huynh-Feldt	29.153	24.000	1.215		
	Lower-bound	29.153	12.000	2.429		
Display * RWL * DH_RVR	Sphericity Assumed	10.036	4	2.509	.537	.709
	Greenhouse-Geisser	10.036	2.376	4.223	.537	.620
	Huynh-Feldt	10.036	3.002	3.343	.537	.660
	Lower-bound	10.036	1.000	10.036	.537	.478
Error(Display*RWL*DH_RVR)	Sphericity Assumed	224.107	48	4.669		
	Greenhouse-Geisser	224.107	28.514	7.859		
	Huynh-Feldt	224.107	36.024	6.221		

	Lower-bound	224.107	12.000	18.676		
Illum * DH_RVR	Sphericity Assumed	1.613	1	1.613	.232	.639
	Greenhouse-Geisser	1.613	1.000	1.613	.232	.639
	Huynh-Feldt	1.613	1.000	1.613	.232	.639
	Lower-bound	1.613	1.000	1.613	.232	.639
Error(Illum*DH_RVR)	Sphericity Assumed	83.373	12	6.948		
	Greenhouse-Geisser	83.373	12.000	6.948		
	Huynh-Feldt	83.373	12.000	6.948		
	Lower-bound	83.373	12.000	6.948		
Display * Illum * DH_RVR	Sphericity Assumed	.549	2	.275	.114	.893
	Greenhouse-Geisser	.549	1.844	.298	.114	.878
	Huynh-Feldt	.549	2.000	.275	.114	.893
	Lower-bound	.549	1.000	.549	.114	.742
Error(Display*Illum*DH_RVR)	Sphericity Assumed	57.981	24	2.416		
	Greenhouse-Geisser	57.981	22.130	2.620		
	Huynh-Feldt	57.981	24.000	2.416		
	Lower-bound	57.981	12.000	4.832		
RWL * Illum * DH_RVR	Sphericity Assumed	7.108	2	3.554	3.234	.057

	Greenhouse-Geisser	7.108	1.463	4.860	3.234	.076
	Huynh-Feldt	7.108	1.615	4.402	3.234	.070
	Lower-bound	7.108	1.000	7.108	3.234	.097
Error(RWL*Illum*DH_RVR)	Sphericity Assumed	26.371	24	1.099		
	Greenhouse-Geisser	26.371	17.551	1.503		
	Huynh-Feldt	26.371	19.375	1.361		
	Lower-bound	26.371	12.000	2.198		
Display * RWL * Illum * DH_RVR	Sphericity Assumed	4.885	4	1.221	.602	.663
	Greenhouse-Geisser	4.885	3.303	1.479	.602	.633
	Huynh-Feldt	4.885	4.000	1.221	.602	.663
	Lower-bound	4.885	1.000	4.885	.602	.453
Error(Display*RWL*Illum*DH_RVR)	Sphericity Assumed	97.376	48	2.029		
	Greenhouse-Geisser	97.376	39.640	2.457		
	Huynh-Feldt	97.376	48.000	2.029		
	Lower-bound	97.376	12.000	8.115		